THE UNIVERSITY of TENNESSEE KNOXVILLE

Day 3. Dimensionality Reduction Methods for Spectral Analysis

Sergei V. Kalinin

Linear Unmixing methods

1. **Why linear unmixing?**
   - Spectral images
   - Image analysis

2. **Multiple linear regression**

3. **Principal component analysis (PCA)**
   - Definition and implementation
   - PCA for scanning tunneling microscopy
   - Physical meaning of PCA: band excitation SPM
   - PCA on imaging data

4. **Independent component analysis (ICA)**

5. **N-FINDR and Bayesian linear unmixing**
   - Mapping phase transitions
   - Image segmentation

Physical constraints in linear models: If solution exists and its unique, doesn’t matter how you find it

Spectroscopic Imaging

Scanning probe microscopy:

- Force-distance curve measurements
- Current-voltage measurements
- Piezoresponse force/electrochemical strain spectroscopy

Electron microscopy:

- Electron Energy Loss Spectroscopy

Optical microscopy:

- Hyperspectral imaging
- Time resolved measurements

Mass-spectrometry:

- Secondary ion MS imaging

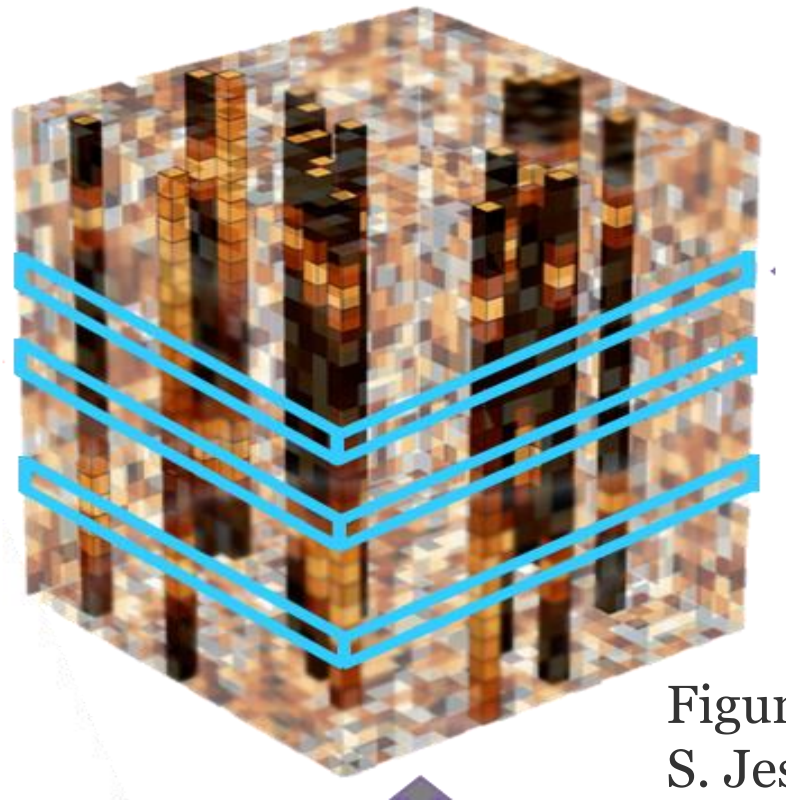

Figure by S. Jesse

In many cases, measured signal can be represented or approximated as a linear combination of signals. However, their functional forms are generally unknown

Very important: convolution with resolution function is also mixing

Physics vs. ML based analysis

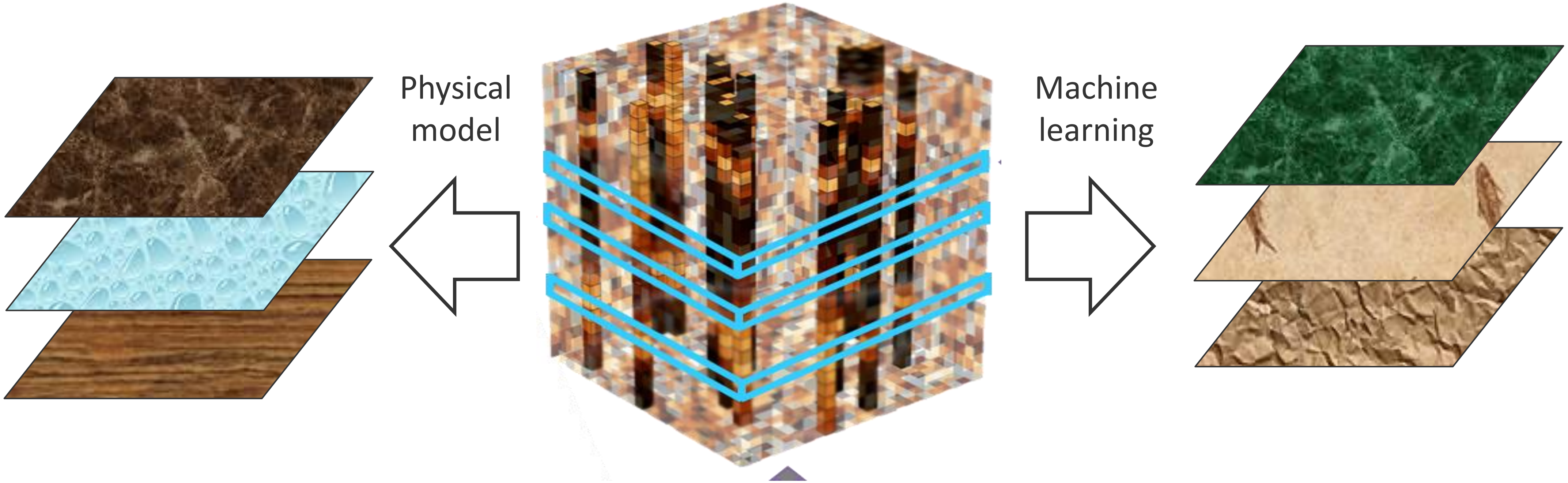

- If we have physical model, we can extract relevant parameters from data
- Imperfect model: epistemic uncertainty
- Noisy data: aleatoric uncertainty
- Analysis results do not depend on sampling of data in x,y

- If we don't have physical model, we can learn intrinsic structure of data
- **Unsupervised learning:** based on data only
  - But not really (definition of distance)
  - Analysis can depend on sampling of data
- **Supervised learning:** based on prior examples
  - Out of distribution shifts

Physics-informed ML: Combines strengths (and limitations) of both

General linear unmixing

$S(\mathbf{x}, \mathbf{R}) = \sum_i a_i(\mathbf{x})\, w_i(\mathbf{R})$+N

We start with:
- $\mathbf{x}$ is the spatial variable, x = (x,y)
- R is the (vector) parameter variable

Overall, for MxM image and P point in spectra, we have M^2P data points

We aim to get:
- $a_i(\mathbf{x})$ are loading maps
- $w_i(\mathbf{R})$ are endmembers/eigenvectors
- N is noise

Overall, we can have (maximum) P loading maps of M^2 size. However, not all of them will have useful information

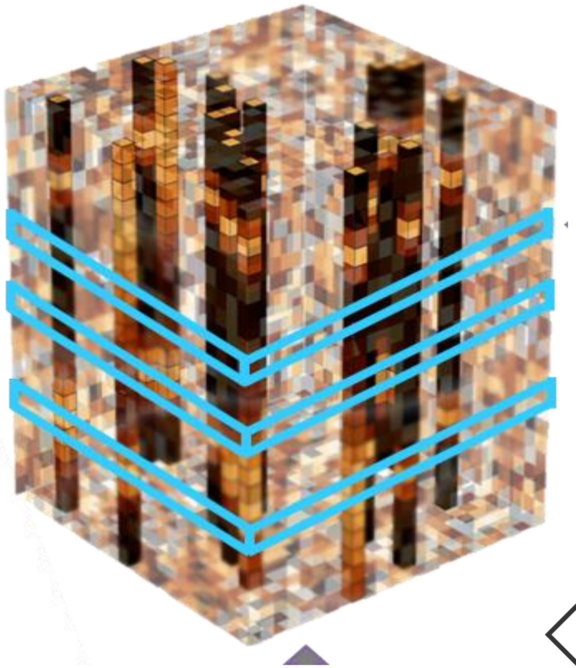

Figure by S. Jesse

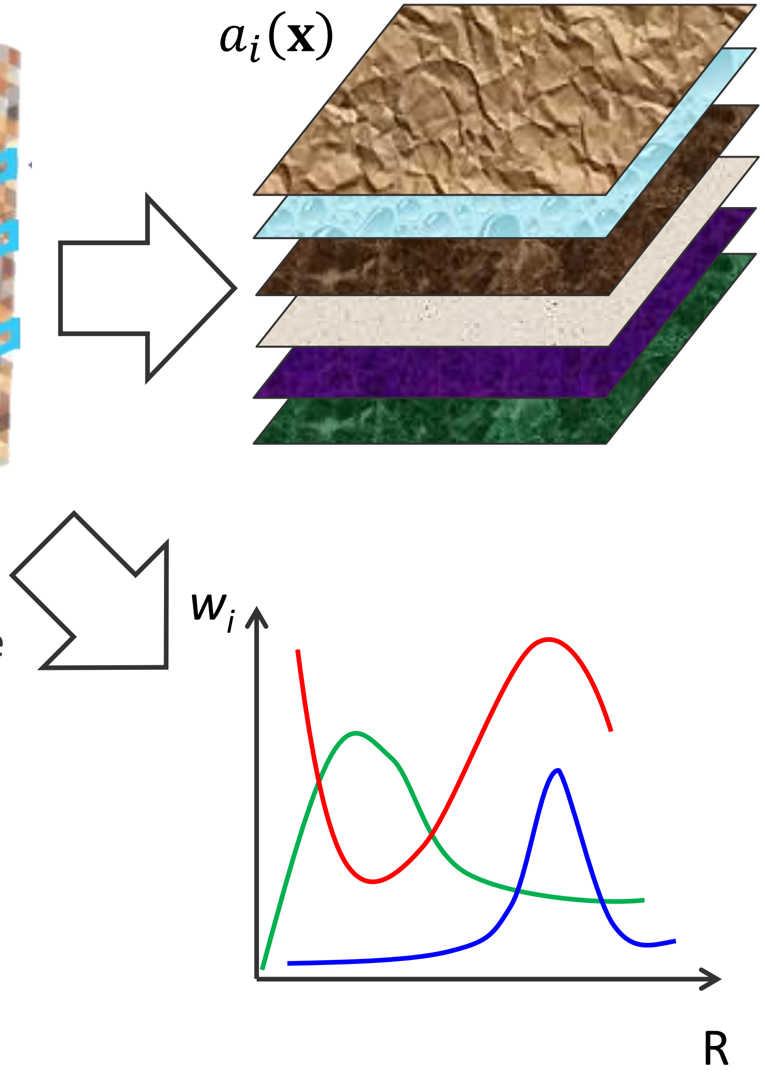

Multiple Linear Regression

Linear mixing $S(\mathbf{x}, \mathbf{R}) = \sum_i \boxed{a_i(\mathbf{x})}\, w_i(\mathbf{R})$ +N but $w_i(\mathbf{R})$ are **known**

STEM of STO/LSMO/BFO interface

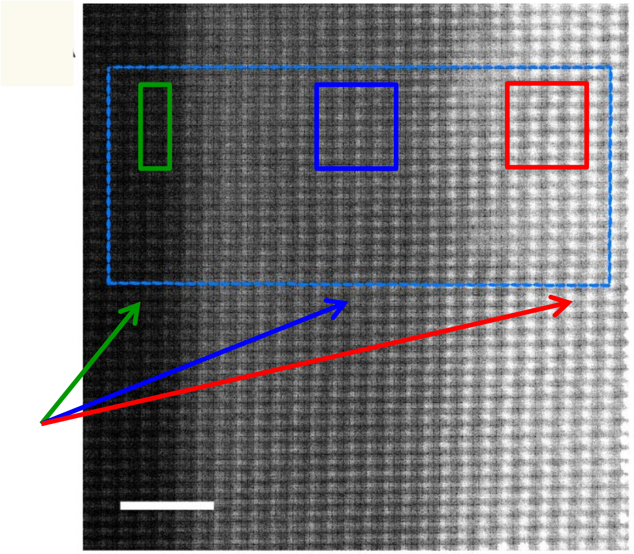

Standard spectra

Low-loss EELS spectra of three components

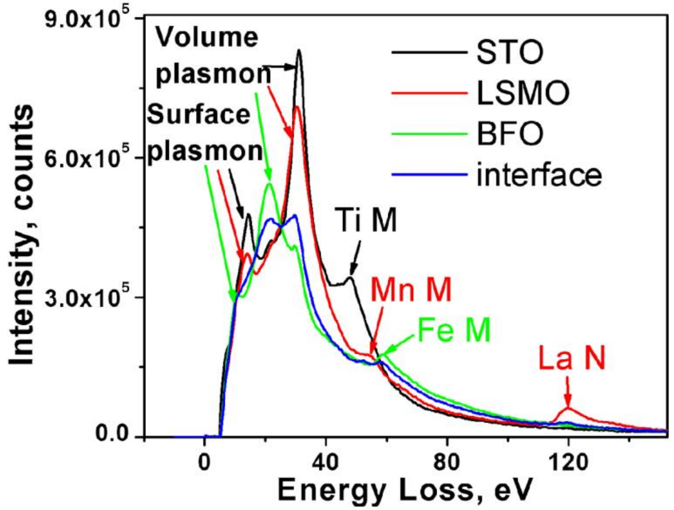

A.Y. BORISEVICH ET AL, *Suppression of Octahedral Tilts and Associated Changes in Electronic Properties at Epitaxial Oxide Heterostructure Interfaces*, Phys. Rev. Lett. **105**, 087204 (2010).

Fit coefficient map **residuals map** **χ2 map**

"Chemistry":
35 to 125 eV

"Plasmons"
5 to 35 eV

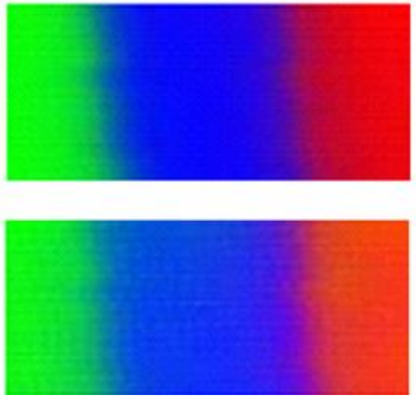

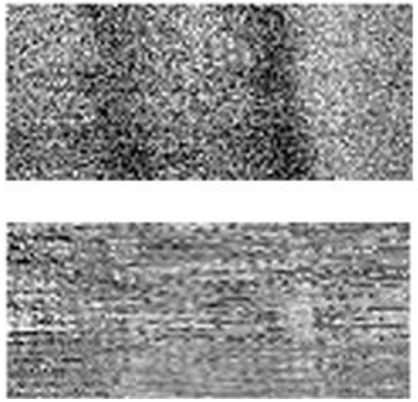

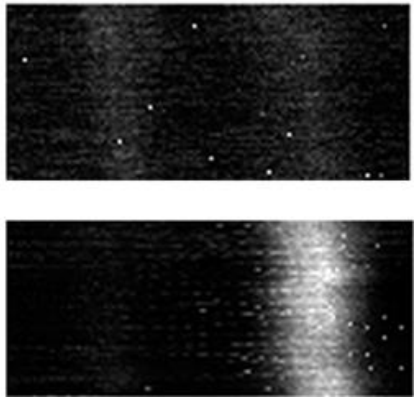

Principal Component Analysis

$$S(\mathbf{x}, \mathbf{R}) = \sum_i a_i(\mathbf{x})\, w_i(\mathbf{R})$$

- In PCA, the eigenvectors $w_i(\mathbf{R})$ are orthonormal and are arranged such that corresponding eigenvalues are placed in descending order by variance
- Can be used to separate "real data" from "noise" – but needs cut-off/selection criteria
- PCA eigenvectors generally do not have defined physical meaning
- PCA is a starting point for many other unmixing methods

Ultramicroscopy 34 (1990) 165–178
North-Holland

EELS elemental mapping with unconventional methods I. Theoretical basis: image analysis with multivariate statistics and entropy concepts

Pierre Trebbia *
Laboratoire de Physique des Solides, Bâtiment 510, F-91405 Orsay Cedex, France

and

Noël Bonnet
Unité INSERM 314 et Université de Reims, 21 rue Clément Ader, F-51100 Reims, France

Received 7 June 1990

Electron energy loss filtered images recorded within a transmission analytical electron microscope are now widely used for the mapping of the elemental distribution of a given atomic species in a specimen prepared as a thin film. Such an image processing may produce both valuable results and artifacts if a careful inspection of all the hypotheses needed by the calculation is not carried out. This paper presents some general statistical methods for a contrast information analysis of a noisy image data set. After a brief introduction of different concepts such as contrast, variance, information and entropy, two unconventional approaches for image analysis are explained: the relative entropy computed with respect to a pure random and signal-free image and the factorial analysis of correspondence (a branch of multivariate statistics). In the companion article (part II), these concepts are applied to real experiments and the results compared with those obtained with a conventional method. Although electron energy loss spectroscopy is the only technique considered here, these methods for image analysis can be applied to a wide variety of noisy data sets (spectra, images, ...) recorded from various sources (electrons, photons, ...).

Why historical papers matter:

1. Often contain elementary introductions
2. Deep insights into principles
3. Surprisingly prescient predictions
4. Comparison with the present: see the big picture

““Those who cannot remember the past are condemned to repeat it.”

George Santayana,
The Life of Reason, 1905

KNOXVILLE

Available online at www.sciencedirect.com

ScienceDirect

ELSEVIER

Ultramicroscopy 106 (2006) 1024–1032

ultramicroscopy

www.elsevier.com/locate/ultramic

Mapping chemical and bonding information using multivariate analysis of electron energy-loss spectrum images

M. Bosman[a,*], M. Watanabe[b], D.T.L. Alexander[c], V.J. Keast[a]

[a]Australian Key Centre for Microscopy and Microanalysis, University of Sydney, Sydney, NSW 2006, Australia
[b]Department of Materials Science and Engineering, Lehigh University, Bethlehem, PA 18015, USA
[c]Department of Materials Science and Metallurgy, University of Cambridge, Pembroke St. CB2 3QZ, UK

Received 23 June 2005; received in revised form 26 October 2005; accepted 18 April 2006

Abstract

Electron energy-loss spectroscopy (EELS) in the transmission electron microscope (TEM) is used to obtain high-resolution information on the composition and the type of chemical bonding of materials. Spectrum imaging, where a full EEL spectrum is acquired and stored at each pixel in the image, gives an exact correlation of spatial and spectral features. However, determining and extracting the important spectral components from the large amount of information contained in a spectrum image (SI) can be difficult. This paper demonstrates that principal component analysis of EEL SIs can be used to extract chemically relevant components. With weighted or two-way scaled principal component analysis, both compositional and bonding information can be extracted. Mapping of the chemical variations in a partially reduced titanium dioxide sample and the orientation-dependent bonding in boron nitride and carbon nanotubes are given as examples.

Why did the PCA on EELS started to grow in 2005 – 2010?

Grain boundary by STM

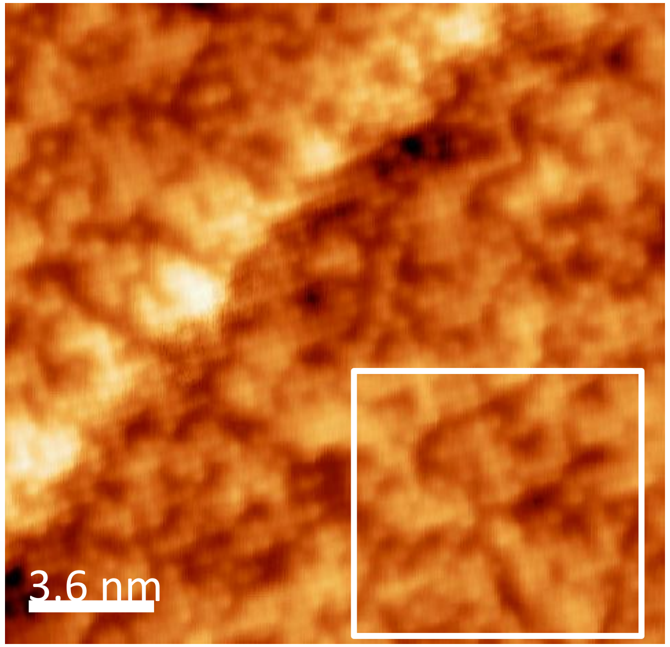

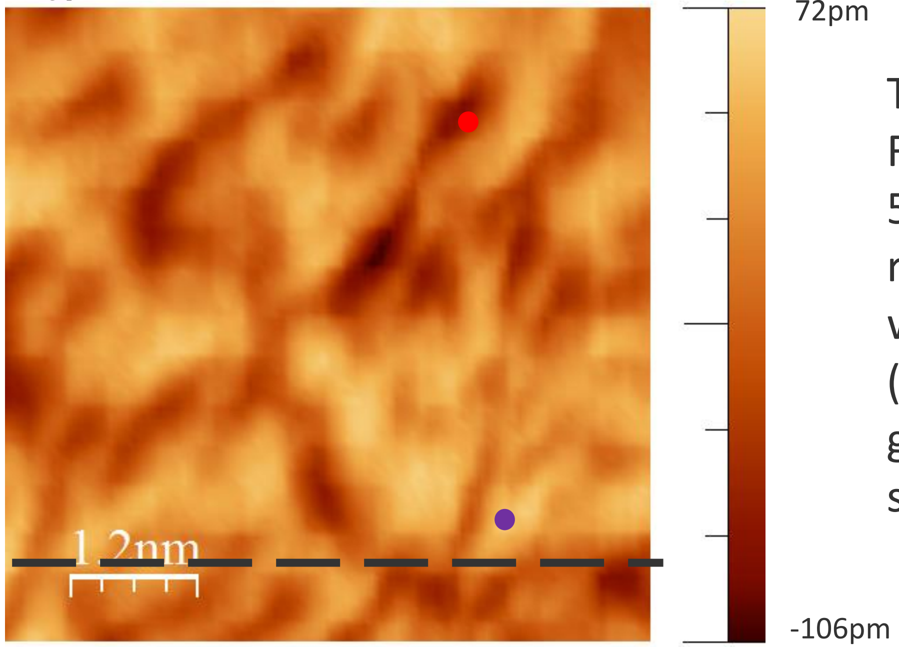

Topographical STM of FeSeTe, T = 82K 15x15nm^2, 50mV, 100pA, white rectangle represents area where CITS was performed; (b) CITS 80x80 pixel graphical average of the spectrographic data.

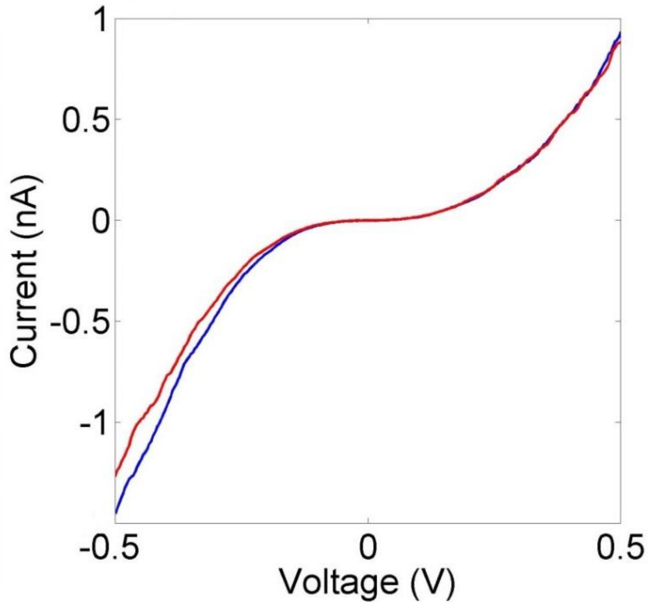

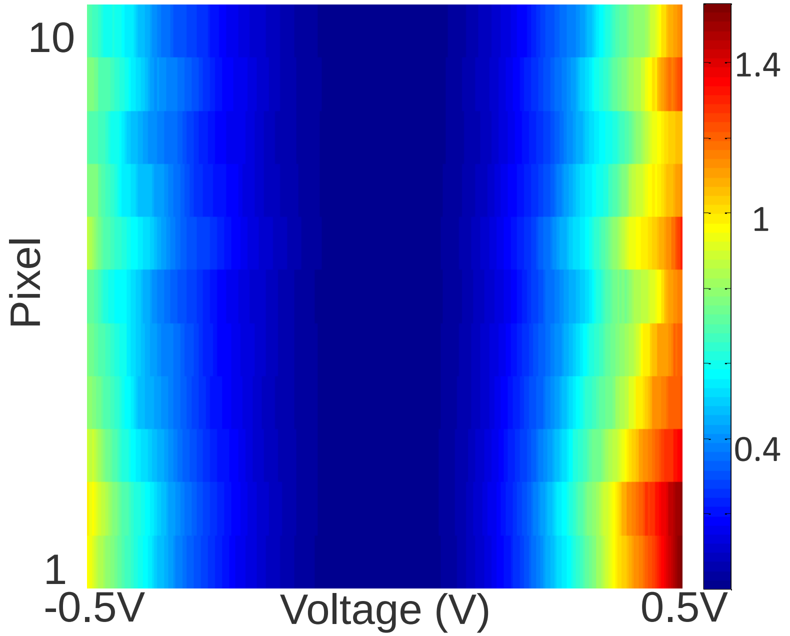

M. Ziatdinov, A. Maksov, L. Li, A. Sefat, P. Maksymovych, and S.V. Kalinin, *Deep data mining in a real space: Separation of intertwined electronic responses in a lightly-doped* $BaFe_2As_2$, Nanotechnology **27**, 475706 (2016).

Eigenvectors and loadings

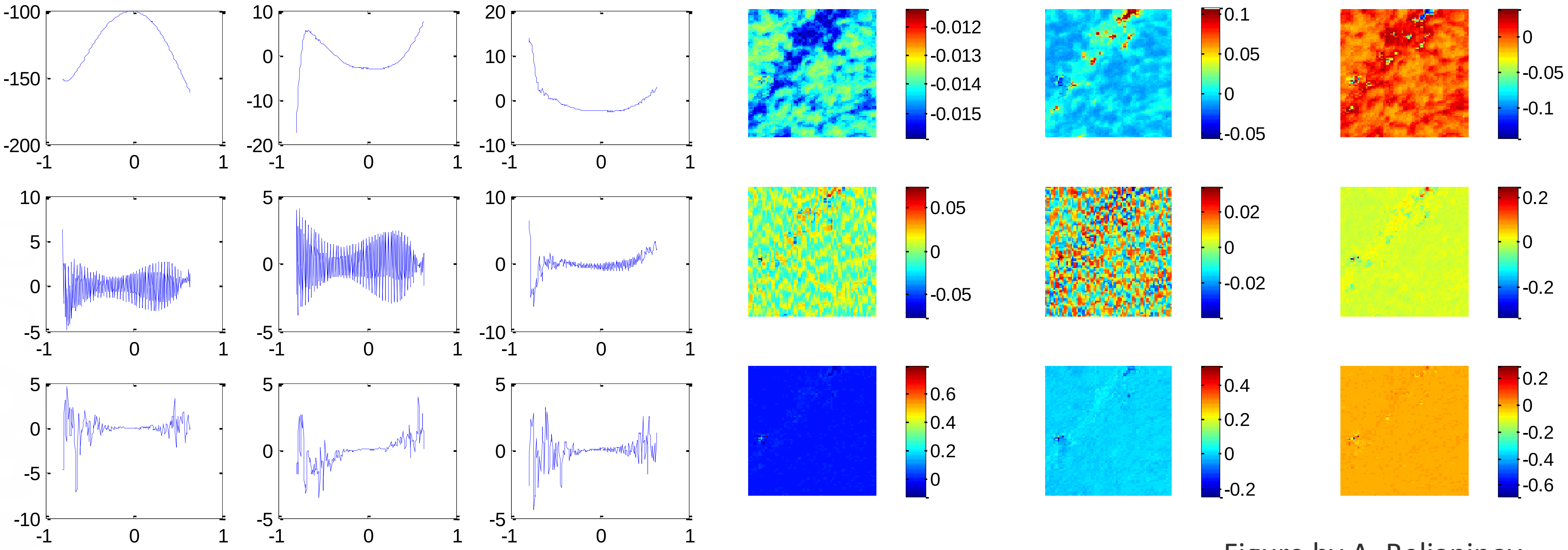

Figure by A. Belianinov

Scree plot and correlations

- Semi log plot indicating the "weight" of each component as a function of all components
- Only the first few components contain useful info, while others are dominated by noise

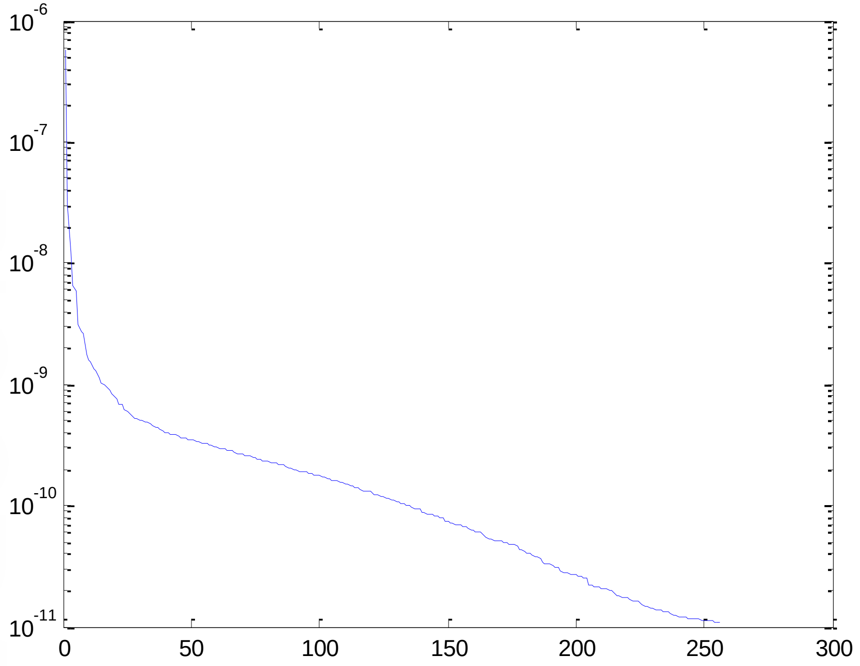

Figure by A. Belianinov

- We can also analyze correlations in images

For AFM data

Spatial correlations

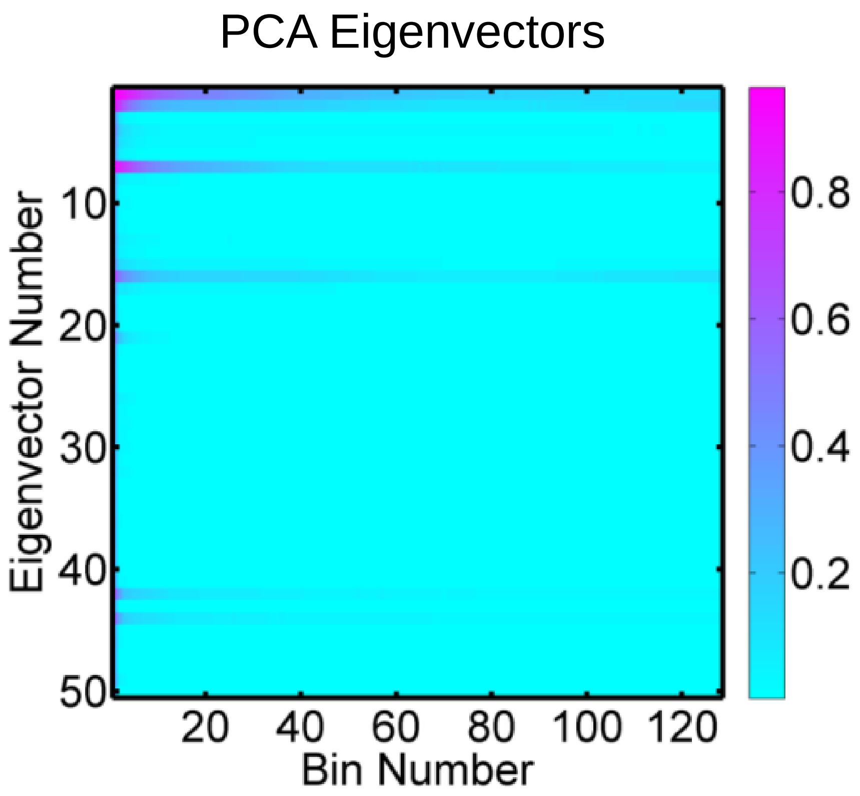

Comparison: PCA vs. functional fit

- Band excitation scanning probe microscopy
- Signal formation mechanism: simple harmonic oscillator

$$A(\omega) = \frac{A^{\max}\omega_0^2}{\sqrt{(\omega^2-\omega_0^2)^2+(\omega\omega_0/Q)^2}}$$

$$\tan(\varphi(\omega)) = \frac{\omega\omega_0/Q}{\omega^2-\omega_0^2}.$$

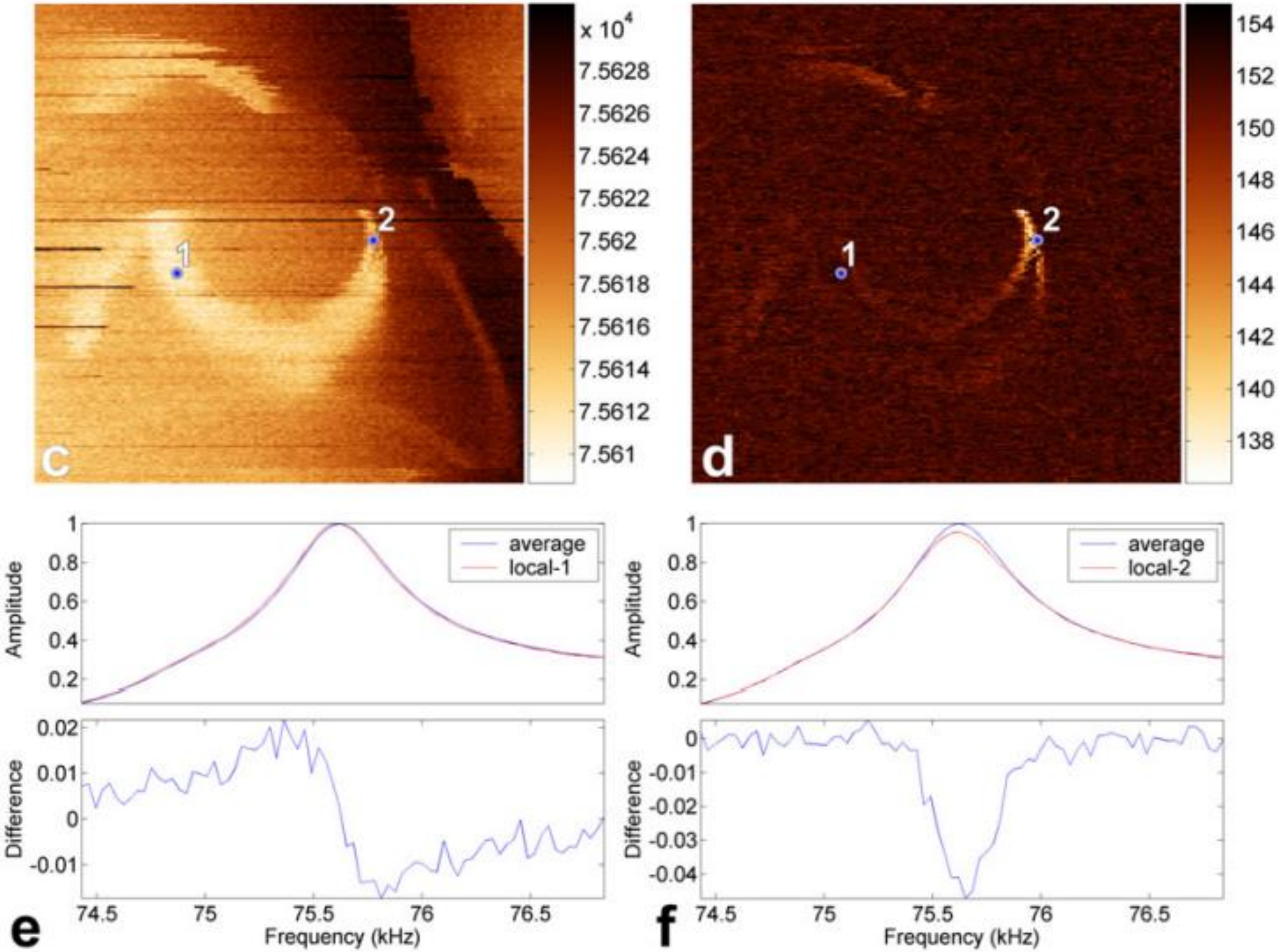

Comparison: PCA vs. functional fit

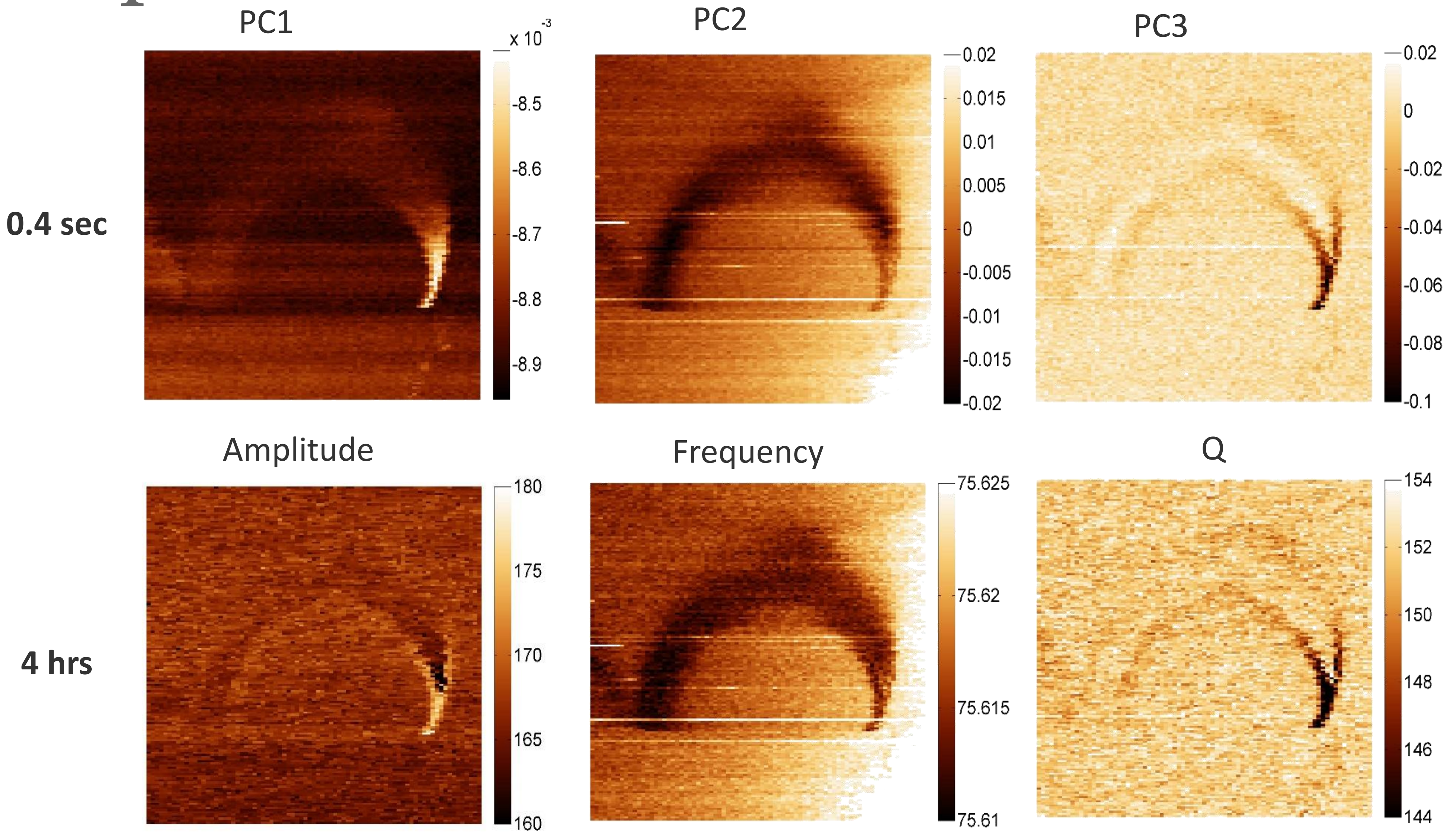

S. JESSE and S.V. KALININ, *Principal component and spatial correlation analysis of spectroscopic imaging data in scanning probe microscopy*, Nanotechnology **20**, 085714 (2009).

When does PCA match physics?

Simulate simple harmonic oscillator curves for different variations of resonance frequency and noise levels

$$A(\omega)=\frac{F\omega\omega_r}{\sqrt{(\omega^2-\omega_r^2)^2+(\omega\omega_r/Q)^2}}+Y(\omega)$$

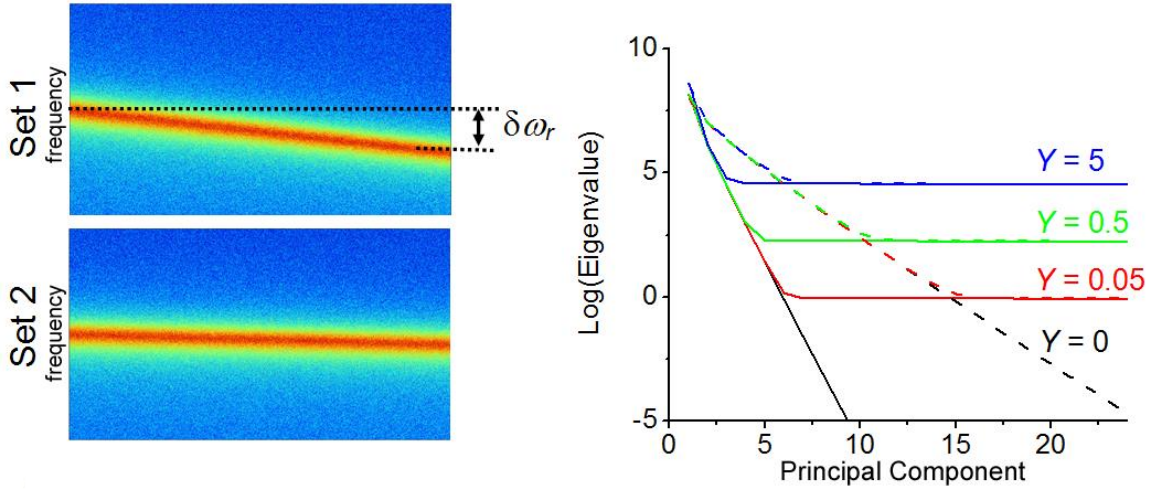

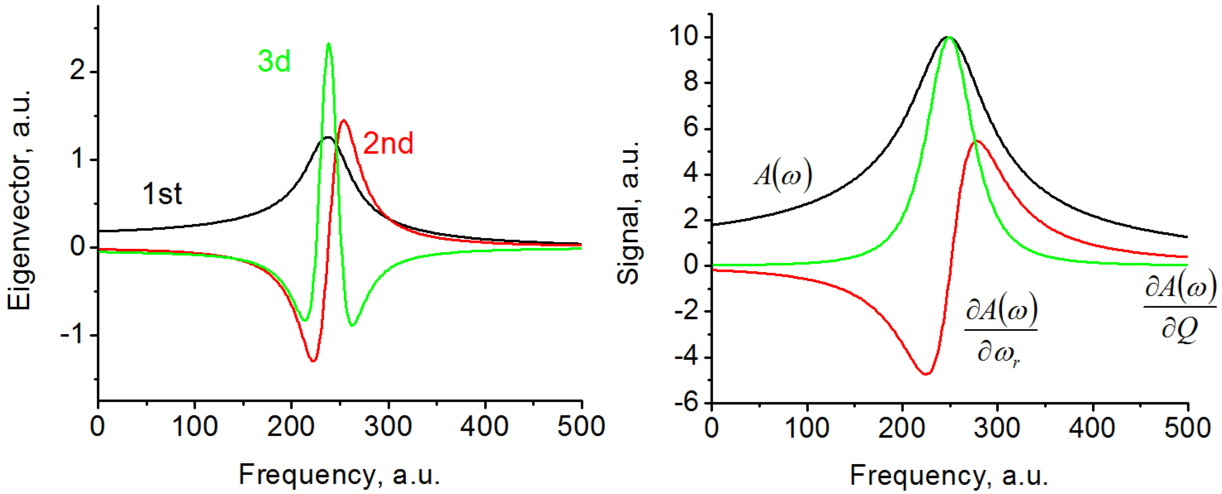

There is similarity between variational derivatives of SHO responses and PCA eigenvectors

$$\delta A_i(\omega)=\frac{\partial A(\omega)}{\partial F}\delta F_i+\frac{\partial A(\omega)}{\partial \omega_r}\delta\omega_{r,i}+\frac{\partial A(\omega)}{\partial Q}\delta Q_i+Y(\omega)$$

S. Jesse and S.V. Kalinin, *Principal component and spatial correlation analysis of spectroscopic imaging data in scanning probe microscopy*, Nanotechnology **20**, 085714 (2009).

K-mean clustering

- PCA is decomposition. But sometimes, we don't want to decompose our signal, but just group them in 'alike' sets.
- This is termed 'clustering'. The easiest and most widely used method is the k-means algorithm

K-means Clustering algorithm, to separate data (x_1,x_2,…,x_n) into *k* clusters

$$\underset{\boldsymbol{S}}{\arg\min} \sum_{i=1}^{k} \sum_{\mathbf{x} \in S_i} \left|\left|\mathbf{x} - \boldsymbol{\mu}_i\right|\right|^2$$

where μ_i is the mean of points in S_i

(Determine **S** = {S_1,S_2,…S_k}, such that within cluster sum of squares is minimized)

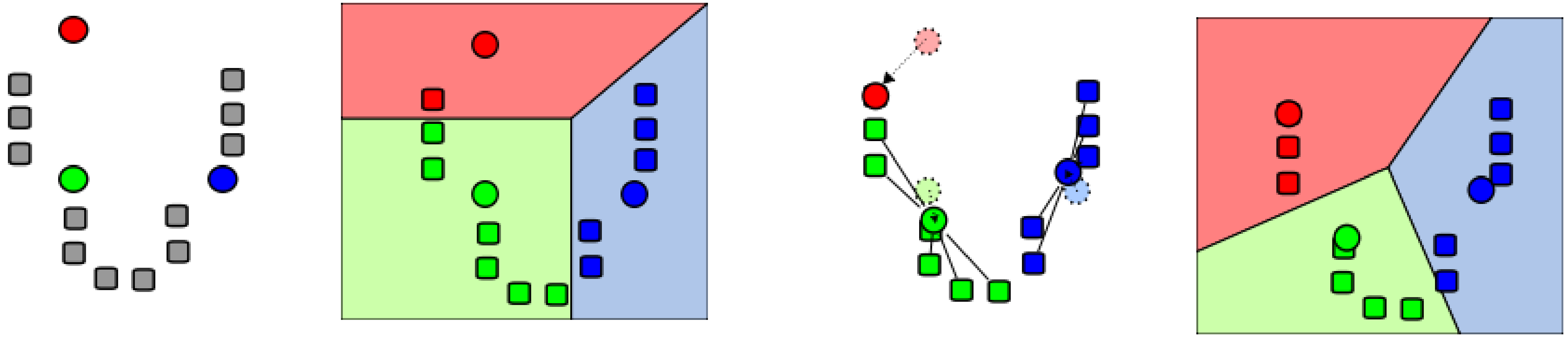

Step 1 Step 2 Step 3 Step 4

Source: Wikipedia

K-means clustering

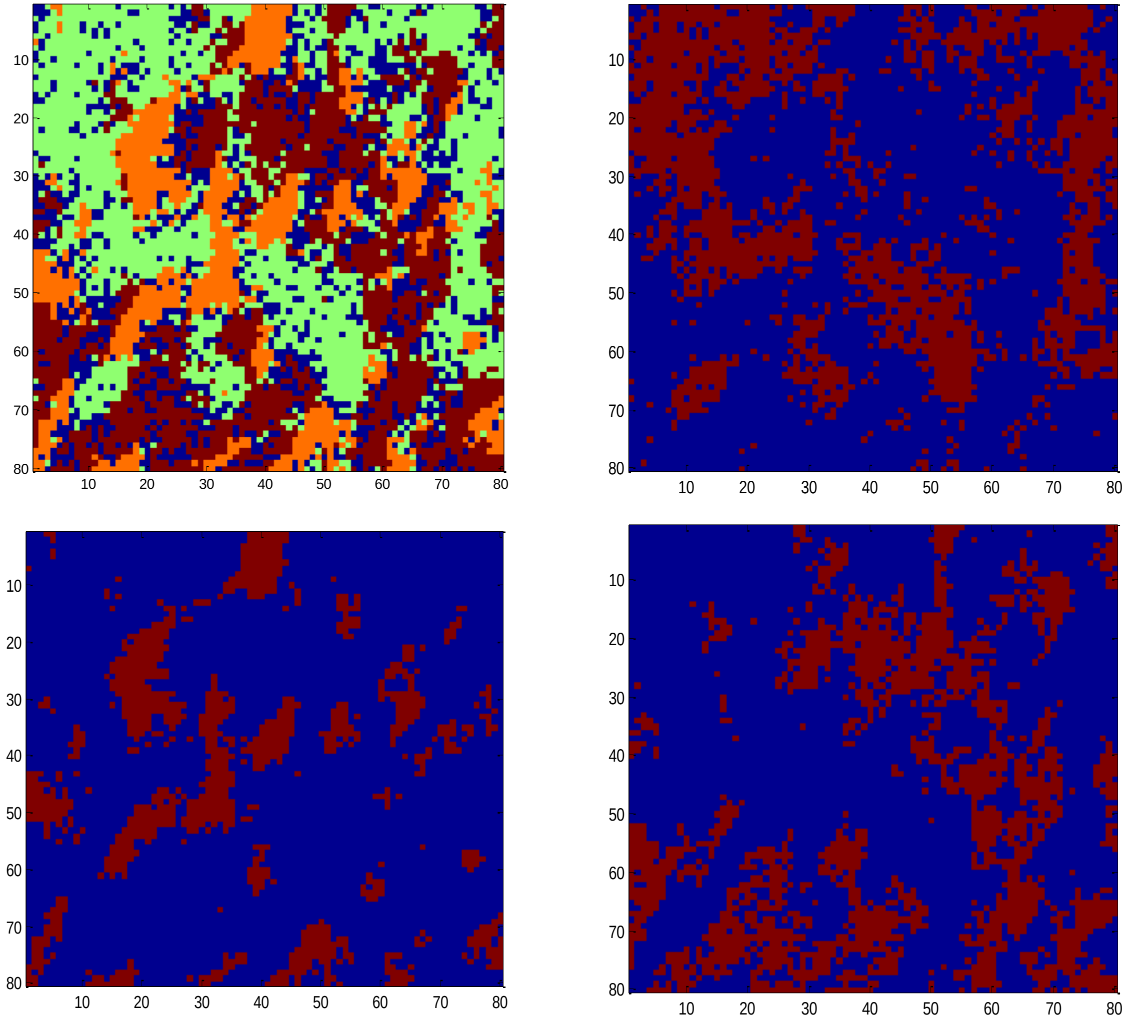

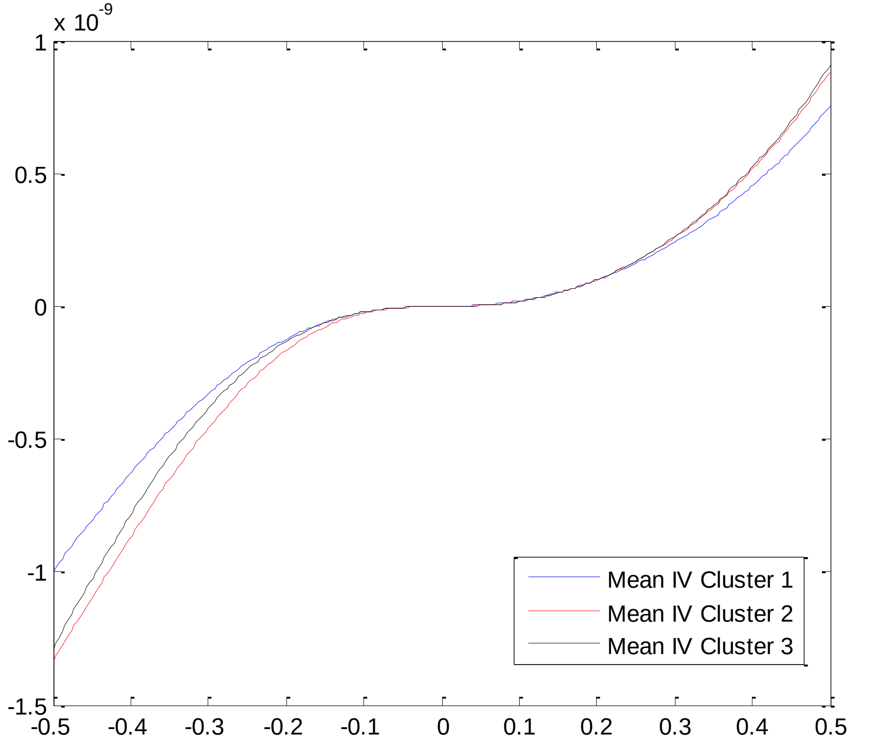

M. Ziatdinov, A. Maksov, L. Li, A. Sefat, P. Maksymovych, and S.V. Kalinin, *Deep data mining in a real space: Separation of intertwined electronic responses in a lightly-doped* $BaFe_2As_2$, Nanotechnology **27**, 475706 (2016).

K-means result of the CITS map broken into
three distinct clusters: CITS map of all three clusters combined vs.
individual cluster distribution in the map

Independent Component Analysis

- **PCA:** orthogonal transformation of possibly correlated variable into a set of linearly uncorrelated variables
  - Analyzes data representing observations described by dependent variables which are inter-correlated
  - Main goal is to find true variables assuming that corrupting noise is Gaussian

- **ICA:** method for separating multivariate signal into additive subcomponents assuming statistical independence of source signals
  - Finds components that are maximally independent and non-Gaussian
  - Blind source separation – cocktail party problem

Compared to PCA, ICA can produce statistically independent non-Gaussian components by decorrelating the higher-order moments in addition to the first- and second-order moments of the statistical distribution

Mathematics of ICA

The Goal is to transform observed data into maximally independent components measured through some function $F(s_1, \ldots, s_n)$ of independence.

- Data as a set of vectors → $x = (x_1, \ldots, x_m)^T$
- Components of the data → $s = (s_1, \ldots, s_n)^T$.

$$s = Wx$$

An observed data vector *x* can then be represented as a sum of independent components *s* weighted by some mixing weight *a*:

$$x_i = a_{i,1}s_1 + \ldots + a_{i,k}s_k + \ldots + a_{i,n}s_n \quad \text{or} \quad x = \sum_{k=1}^{n} s_k a_k$$

In other words, data vector *x* is represented by basis vectors $a_k = (a_{1,k}, \ldots, a_{m,k})^T$

that can form columns of a mixing matrix such that: $x = As$

https://en.wikipedia.org/wiki/Independent_component_analysis

Mathematics of ICA - 2

$$x = As$$

Given that our data is set of vectors *x*, we want to find both, the mixing matrix *A* and sources *s*

This can be done by calculating *w* vectors and a cost function that can maximize the Non-Gaussianity, or minimize mutual information of

$$s_k = (w^T * x)$$

Original sources can then be recovered by multiplying observed data vectors *x* with the inverse of the mixing matrix: $W = A^{-1}$

- Not as easy to utilize as PCA, but excellent premade algorithms are readily available, e.g. Aapo Hyvärinen – FastICA*

http://cis.legacy.ics.tkk.fi/aapo/papers/IJCNN99_tutorialweb/IJCNN99_tutorial3.html
http://research.ics.aalto.fi/ica/fastica/

PCA vs. ICA

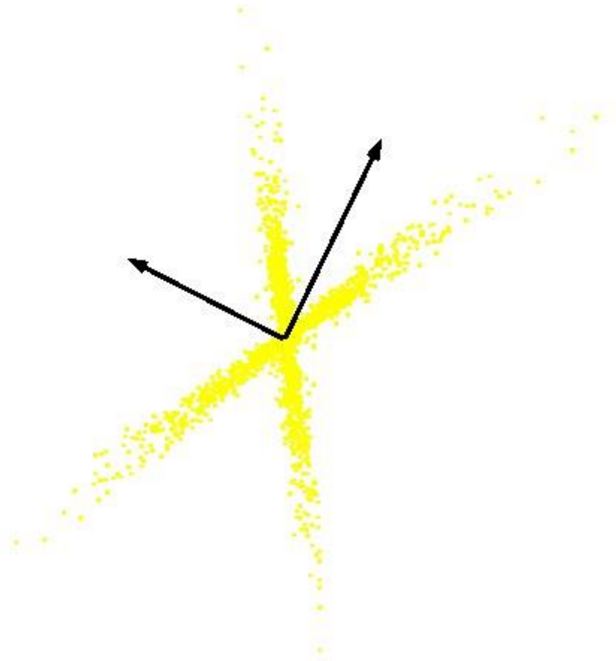

PCA
(orthogonal coordinate)

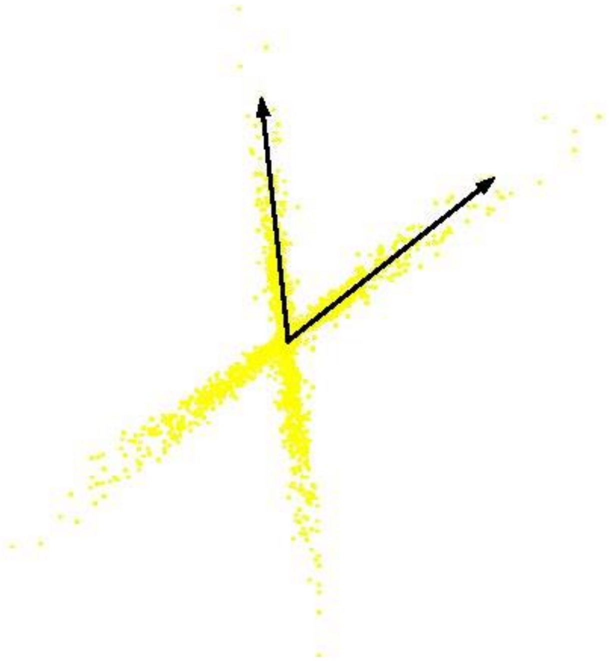

ICA
(non-orthogonal coordinate)

Cocktail Party Problem

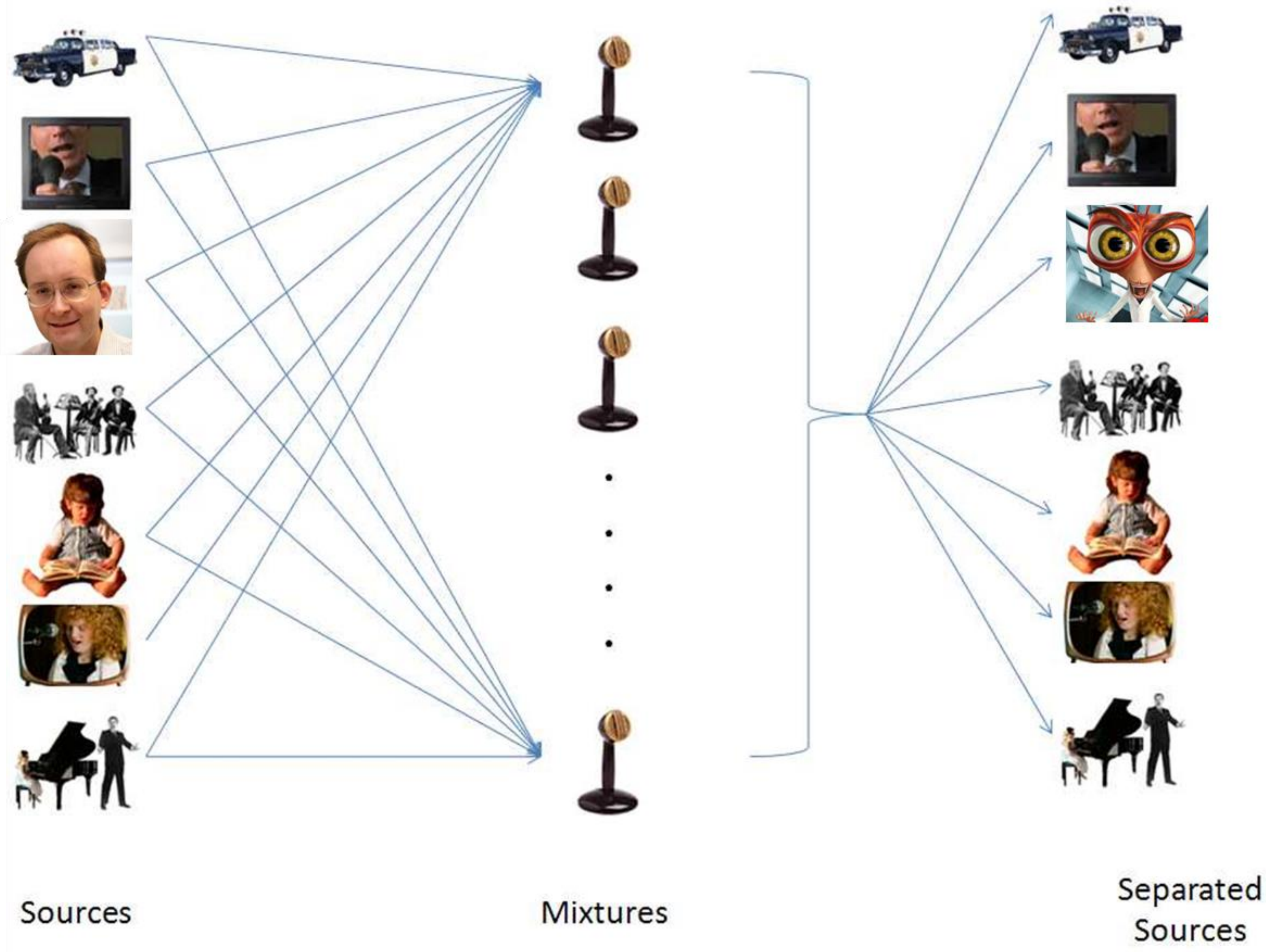

ICA Example

$$\left(R_1(t), R_2(t), \ldots R_n(t)\right)$$

Sources

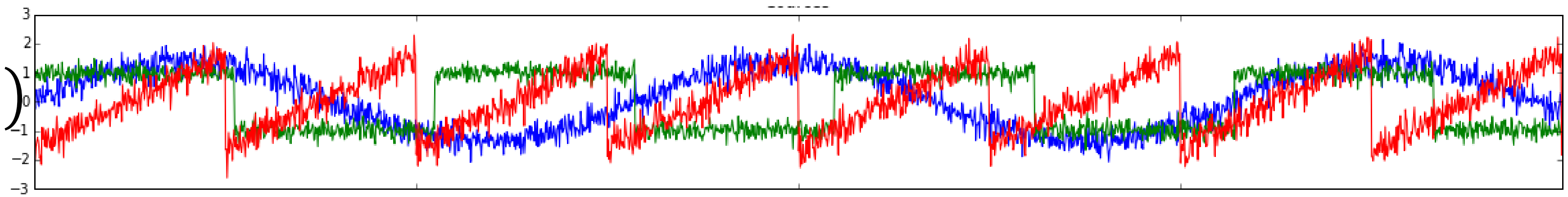

Observations

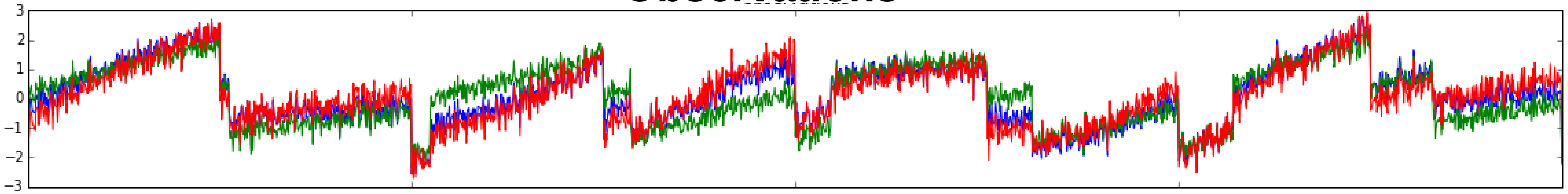

PCA Components

Components are maximally independent

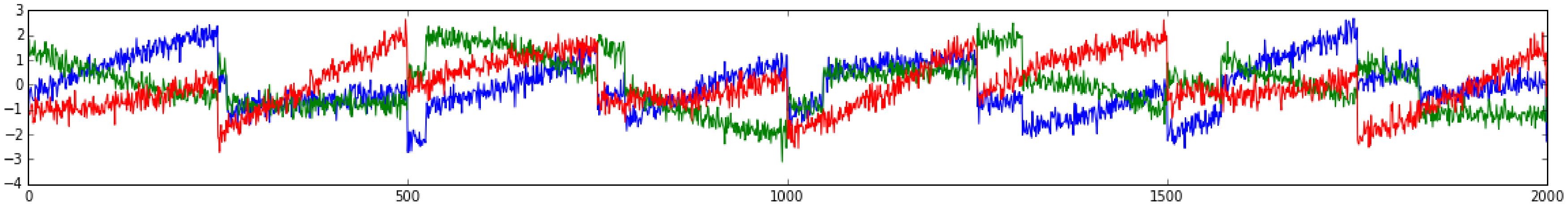

ICA Components

$$\begin{pmatrix} R_1(t) \\ \ldots \\ R_n(t) \end{pmatrix} = \boldsymbol{A} \begin{pmatrix} s_1(t) \\ \cdots \\ s_n(t) \end{pmatrix}$$

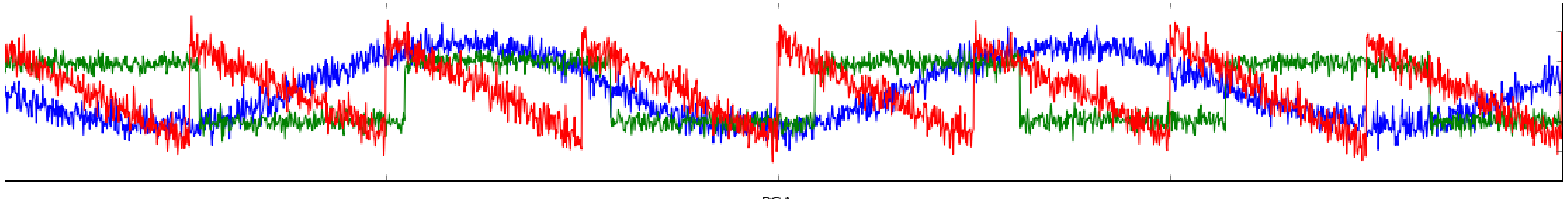

Bayesian Linear Unmixing

$$S(\mathbf{x}, \mathbf{R}) = \sum_{i=1}^{K} a_i(\mathbf{x}) w_i(\mathbf{R}) + \mathrm{N}$$

$$\sum_{i=1}^{K} a_i(\mathbf{x}) = 1$$

- The eigenvectors $w_i(\mathbf{R})$ are non-negative, $w_i(\mathbf{R}) \geq 0$
- The loading coefficients sum to 1
- The number of eigenvectors, K, is a priori unknown

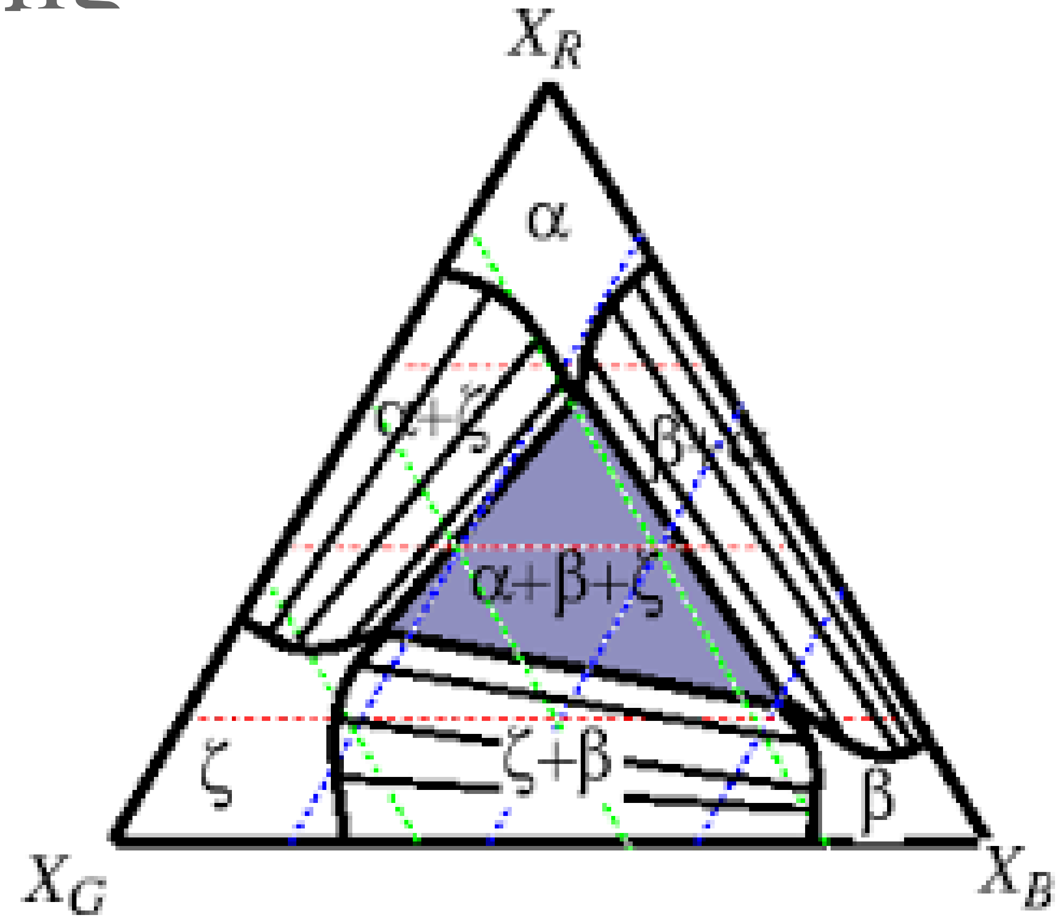

BLU is ideally suited for certain classes of problems, e.g. conduction through parallel channels, optical or electronic spectra of mixtures, etc

Laser heating induced phase transitions

- Copper indium thiophosphate ($Cu_{0.77}In_{1.12}P_2S_6$) layered ferroelectric
  - Ferroelectric state at room temperature
  - Curie temperature T_c = 320 K
  - Non-polar $In_{4/3}P_2S_6$ inclusions

- Combined Atomic Force Microscopy (AFM) and confocal Raman spectroscopy investigative approach
  - AFM – topography measurements
  - Piezoresponse force microscopy (PFM) – static ferroelectric domain structure
  - Raman – crystallographic structure via Raman spectra

Experimental scheme

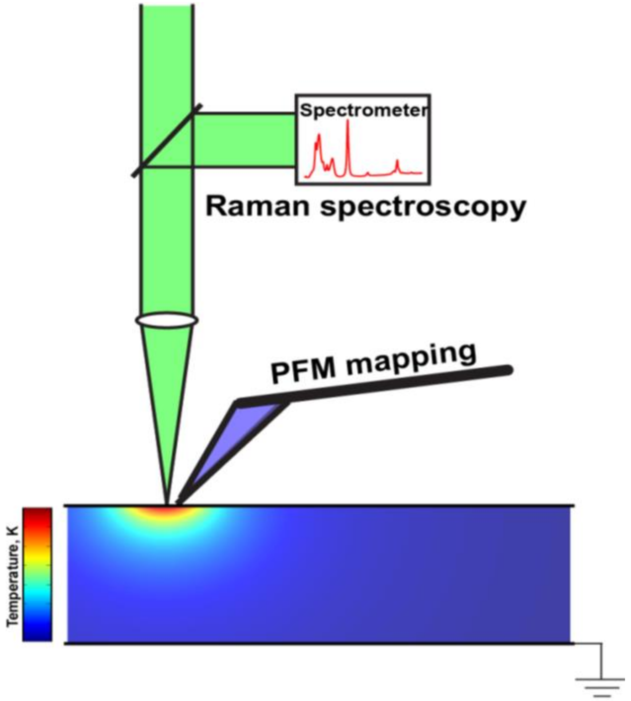

Ferroelectric domain structure

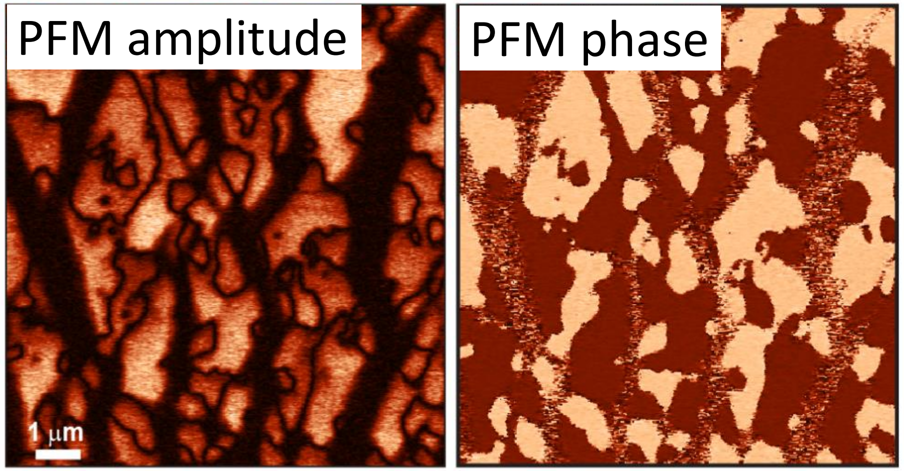

Single point Raman spectra

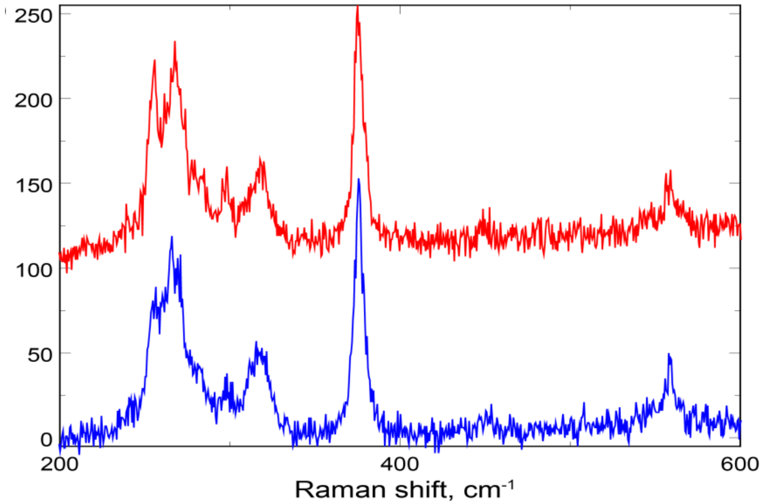

A. IEVLEV, ACS Nano **9**, 12442 (2015).

Laser heating induced phase transition

Laser can be used for local heating to induce ferroelectric- paraelectric phase transition

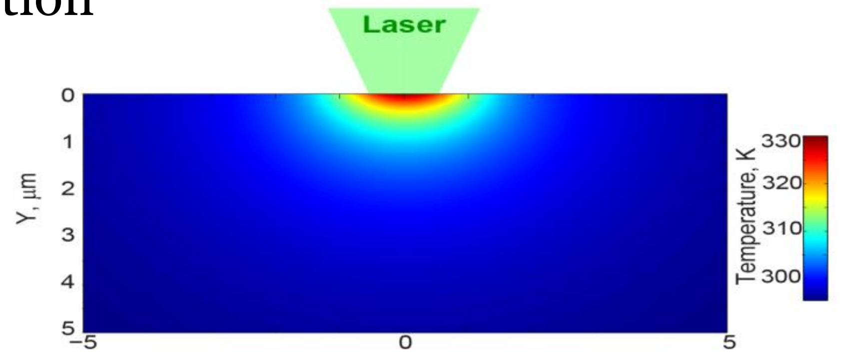

Domain structure evolution

Laser power

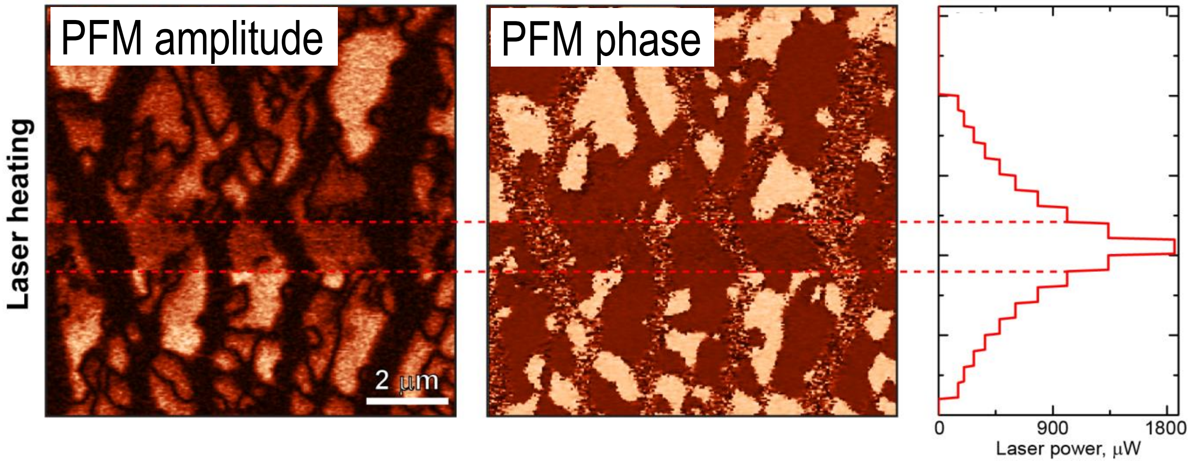

- Measurements with variation of the laser power
  - PFM – *in-situ* change in the domain structure above T_c
  - Raman – evolution of the Raman spectra through the phase transition
- Comprehensive analysis of Raman spectra is complicated by inhomogeneous chemical composition and high noise level
- Bayesian Linear Unmixing can be used for automated identification of spectra evolution

Raman spectra evolution (averaged)

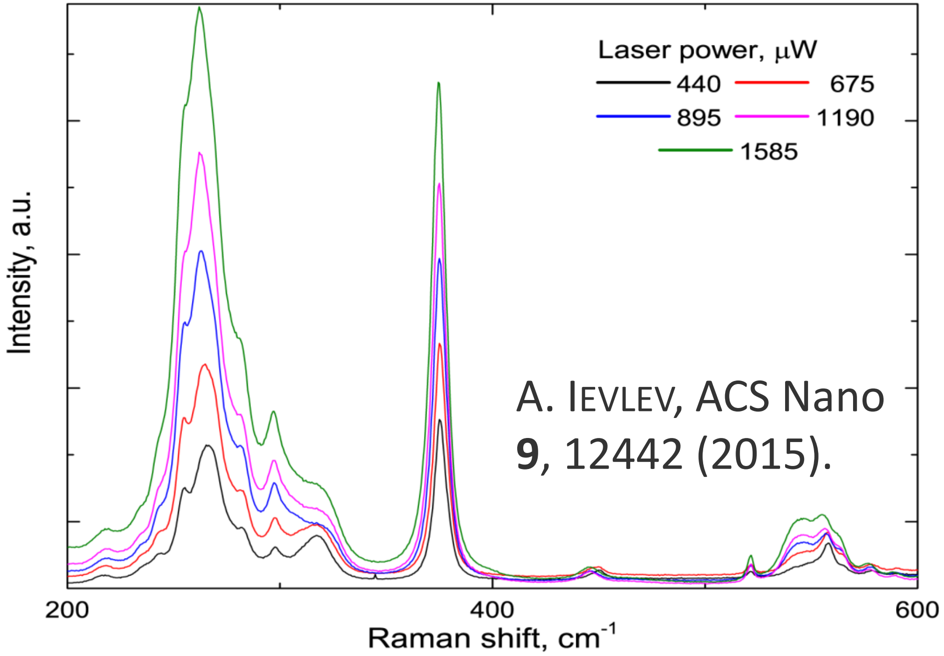

A. Ievlev, ACS Nano **9**, 12442 (2015).

BLU separation of components

Spatial concentration of components

Results of BLU: components and loading maps

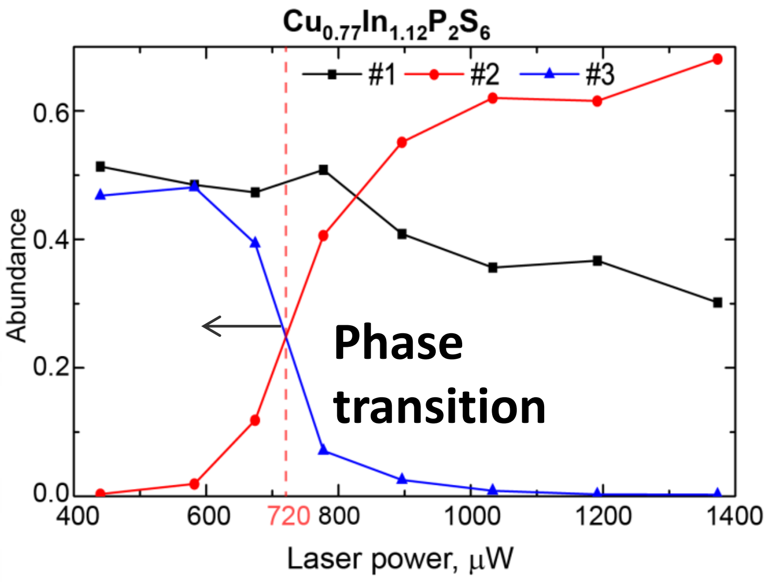

A. IEVLEV, ACS Nano **9**, 12442 (2015).

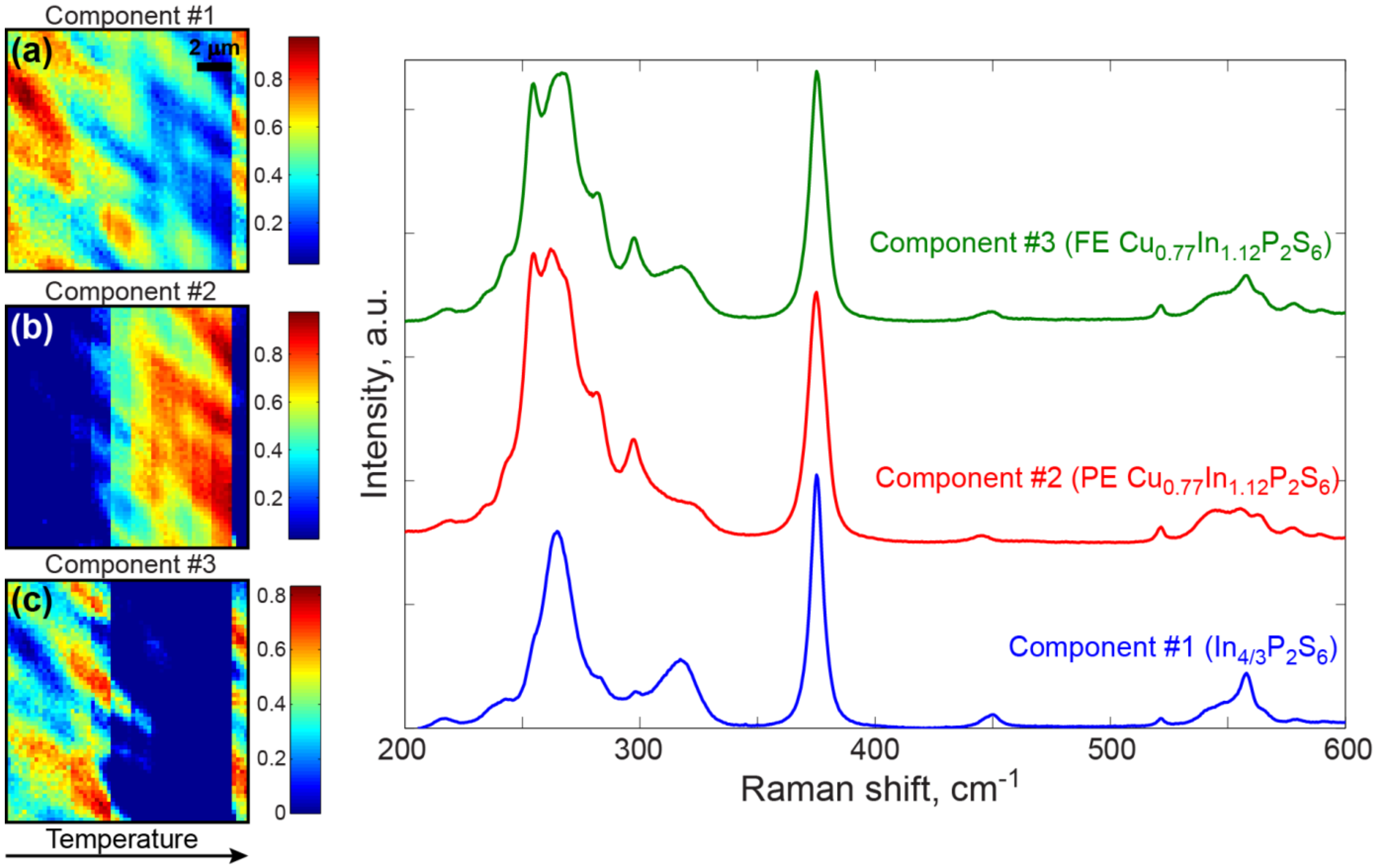

Unmixing showed presence of three independent components in Raman spectra:

1. Non-polar $In_{4/3}P_2S_6$ – weak changes in intensity with temperature
2. Paraelectric $CuInP_2S_6$ above T_c – appears at higher laser powers
3. Ferroelectric $CuInP_2S_6$ below T_c – disappears at higher temperatures

Day3_PCA_CL.ipynb

First order reversal curve IV measurements

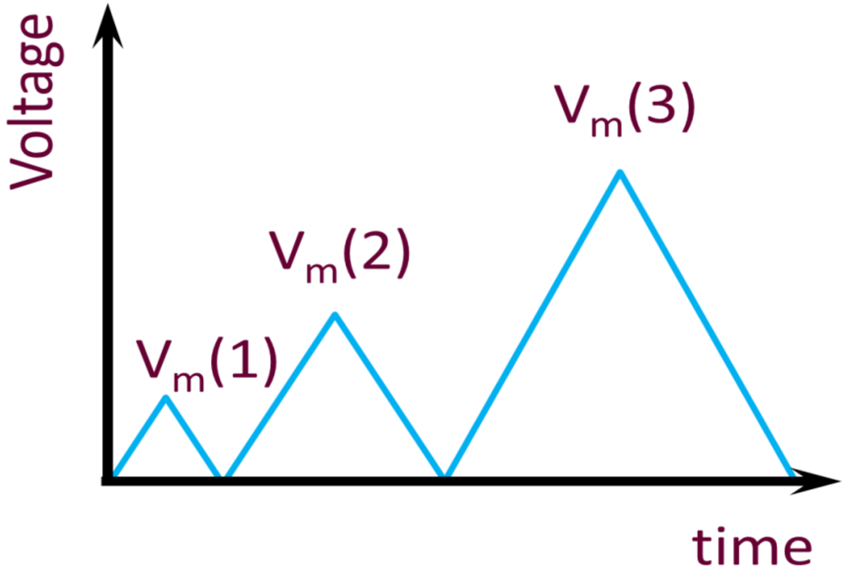

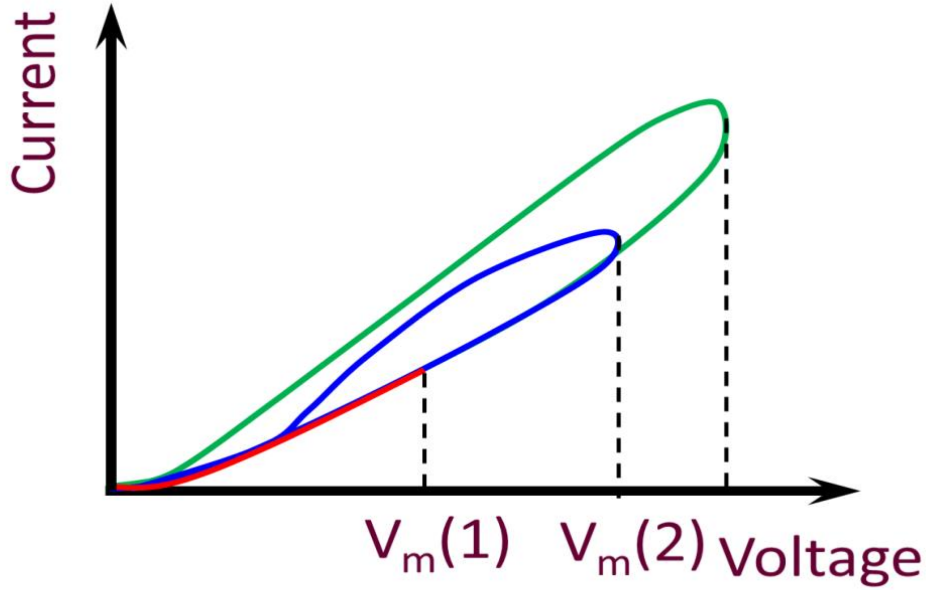

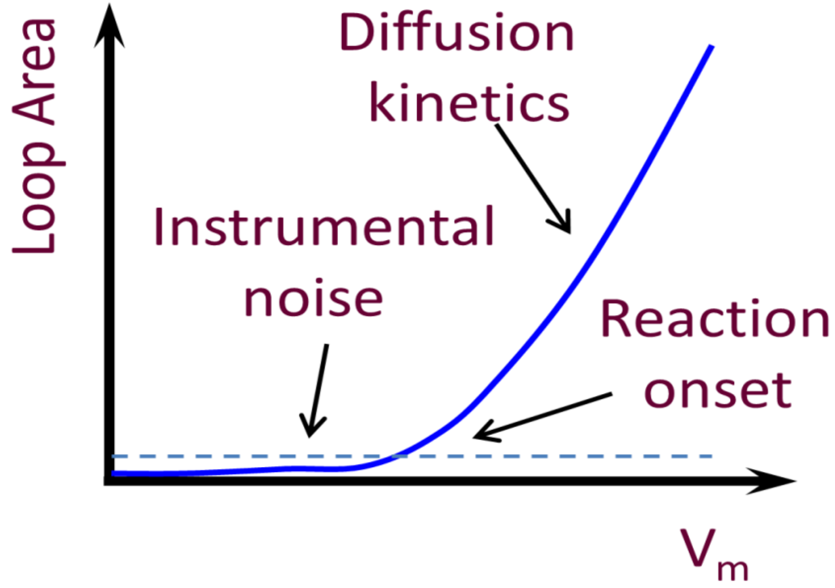

- First order reversal curves in IV measurements
- Opening of hysteresis loops indicates onset of slow-bias-induced changes
- These can be explored as a function of rate and bias

Conductance in nanotubular structures

Probing electrochemistry through electronic degrees of freedom

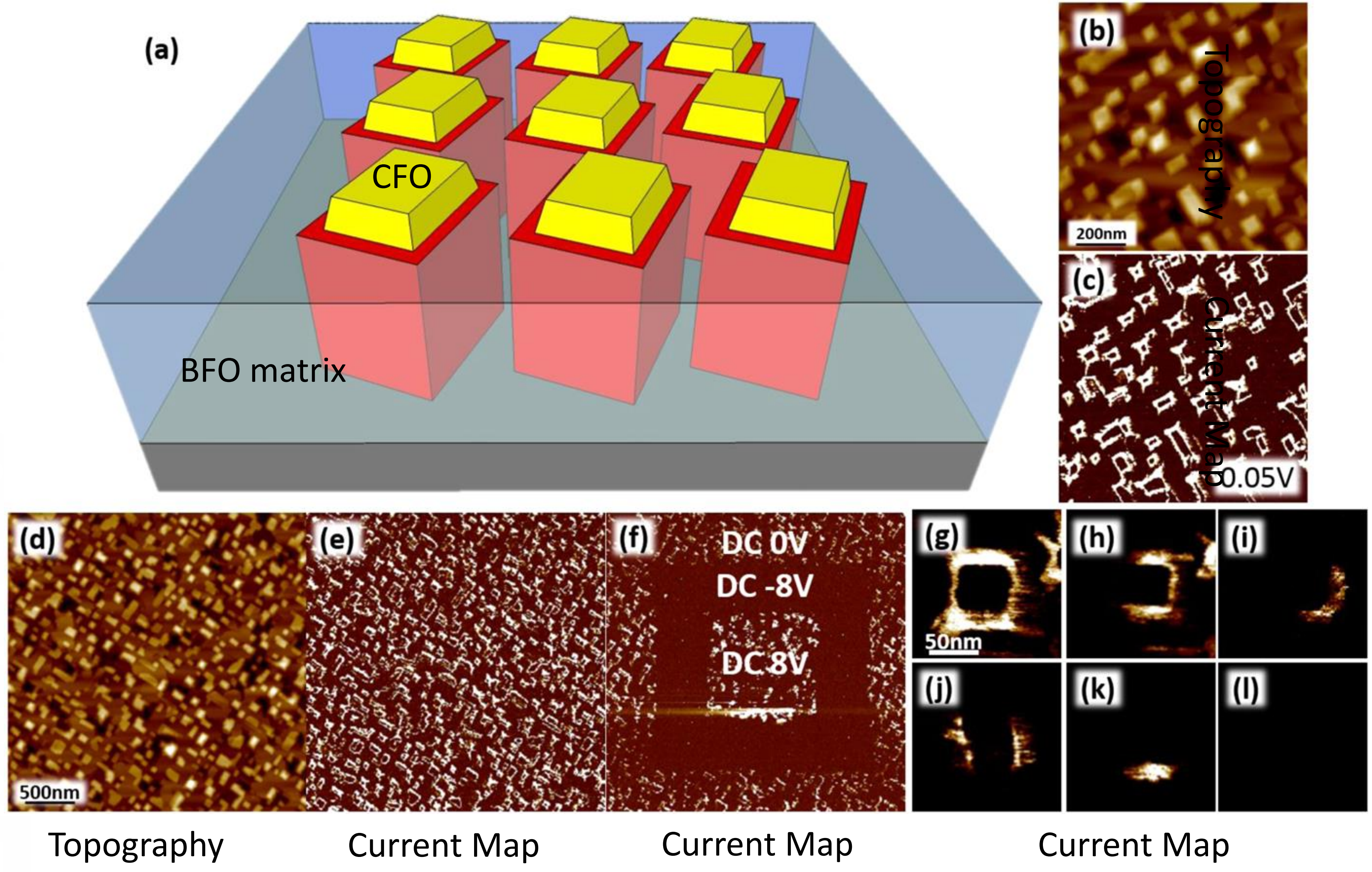

Y.H. Hsieh, E. Strelcov, J.M. Liou, C.Y. Shen, Y.C. Chen, S.V. Kalinin, and Y.H. Chu, *Electrical Modulation of the Local Conduction at Oxide Tubular Interfaces*, ACS Nano **7**, 8627 (2013).

FORC IV of BFO-CFO

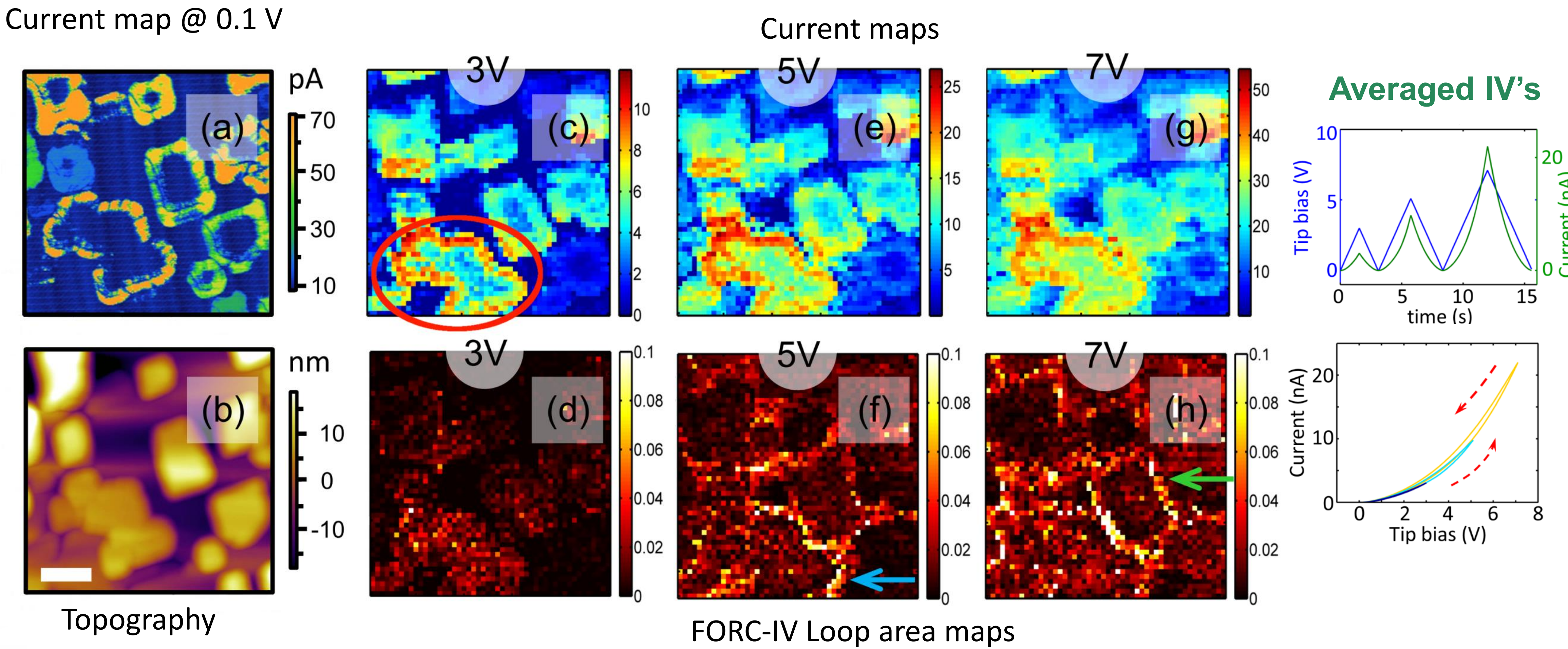

- Clear variability of conductance and loop opening behavior
- "Too much data" – FORC IV loops that can be reduced to multiple current and loop opening maps as a function of peak voltage

E. STRELCOV ET AL, ACS Nano **8**, 6449 (2014).

Bayesian linear unmixing

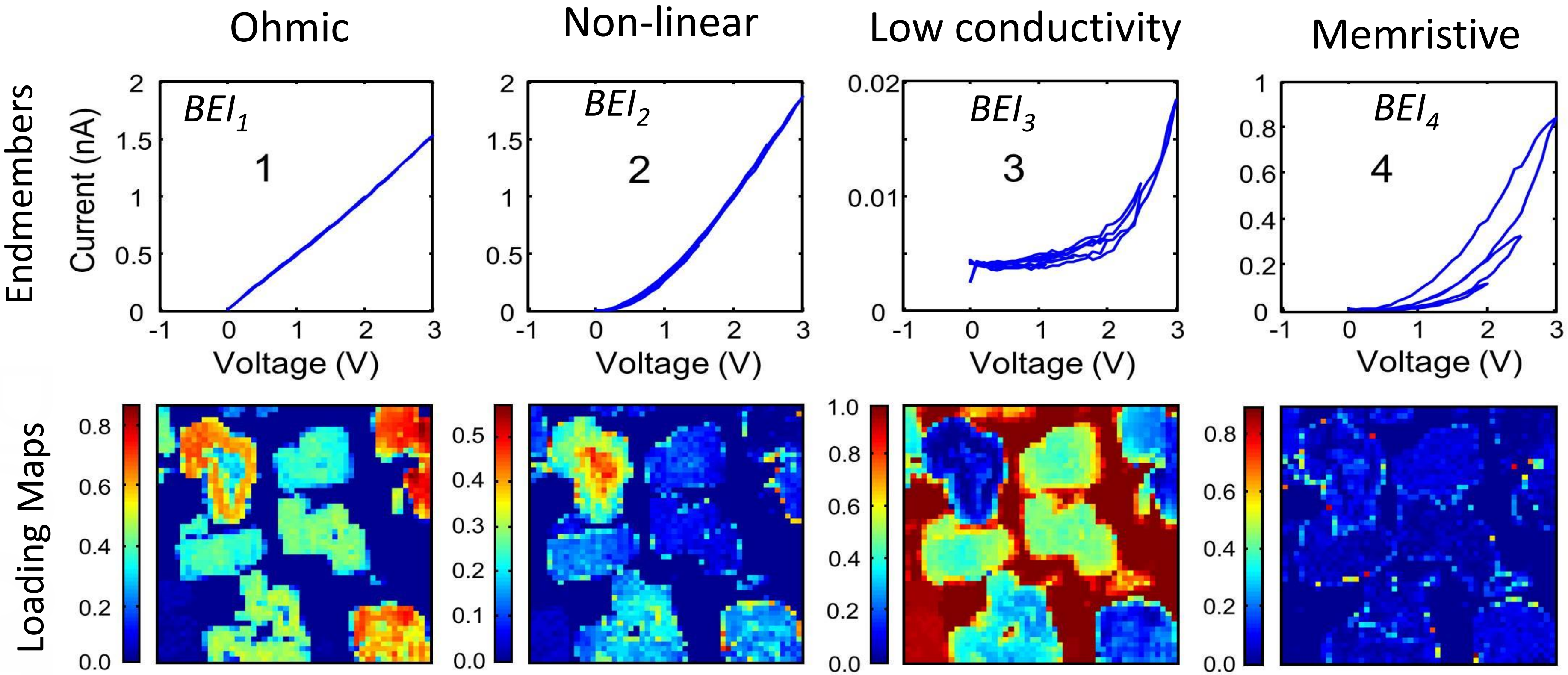

E. Strelcov, A. Belianinov, Y.H. Hsieh, S. Jesse, A.P. Baddorf, Y.H. Chu, and S.V. Kalinin, *Deep Data Analysis of Conductive Phenomena on Complex Oxide Interfaces: Physics from Data Mining*, ACS Nano **8**, 6449 (2014).

Separates 4 different types of behavior, all making physical sense. Loading maps normalized to unity.

$$I_{xy} = \sum_{j}^{n} I_{xyj} = \sum_{j}^{n} \alpha_{xyj} BEI_j \qquad \sum_{j}^{n} \alpha_{xyj} = 1$$

Fit to physical models

Mechanism\ Endmember	Fowler-Nordheim	Poole-Frenkel	Schottky	Mott-Gurney	Child's Law
1st	-	-	-	-	-
2nd	good†	bad	bad	good	good
3rd	fair†	bad	bad	bad	bad
4th forward	bad	good†	bad	bad	bad
4th reverse	good†	bad	fair	bad	bad

†The values of the fitting coefficients are physically meaningful

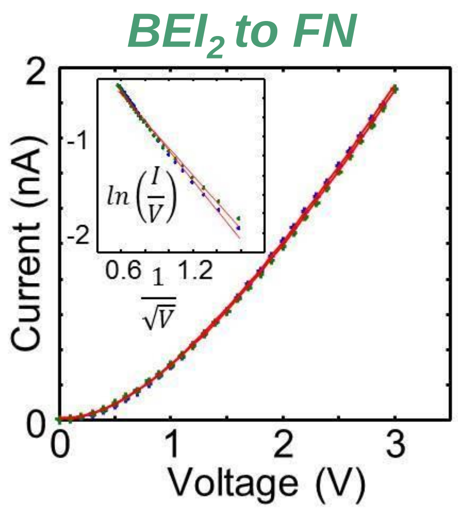

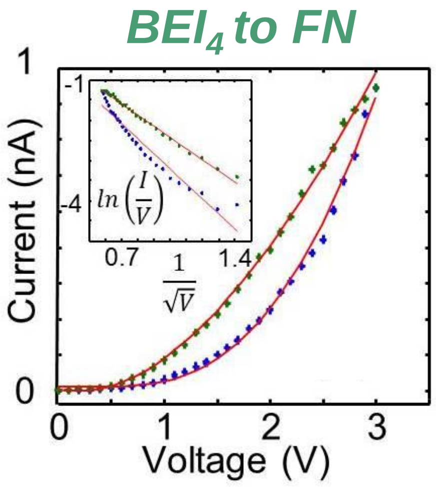

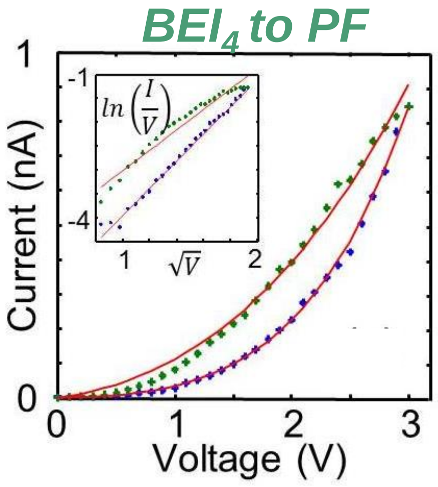

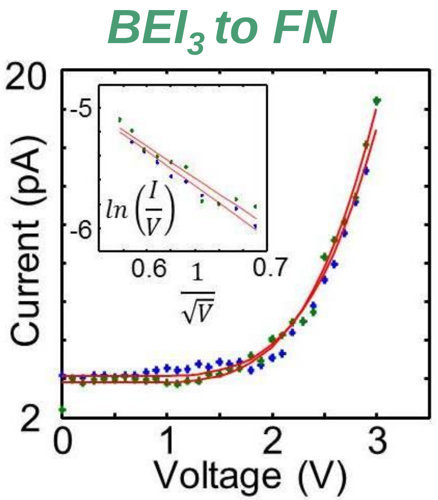

E. Strelcov, A. Belianinov, Y.H. Hsieh, S. Jesse, A.P. Baddorf, Y.H. Chu, and S.V. Kalinin, *Deep Data Analysis of Conductive Phenomena on Complex Oxide Interfaces: Physics from Data Mining*, ACS Nano **8**, 6449 (2014).

FORC IV workflow

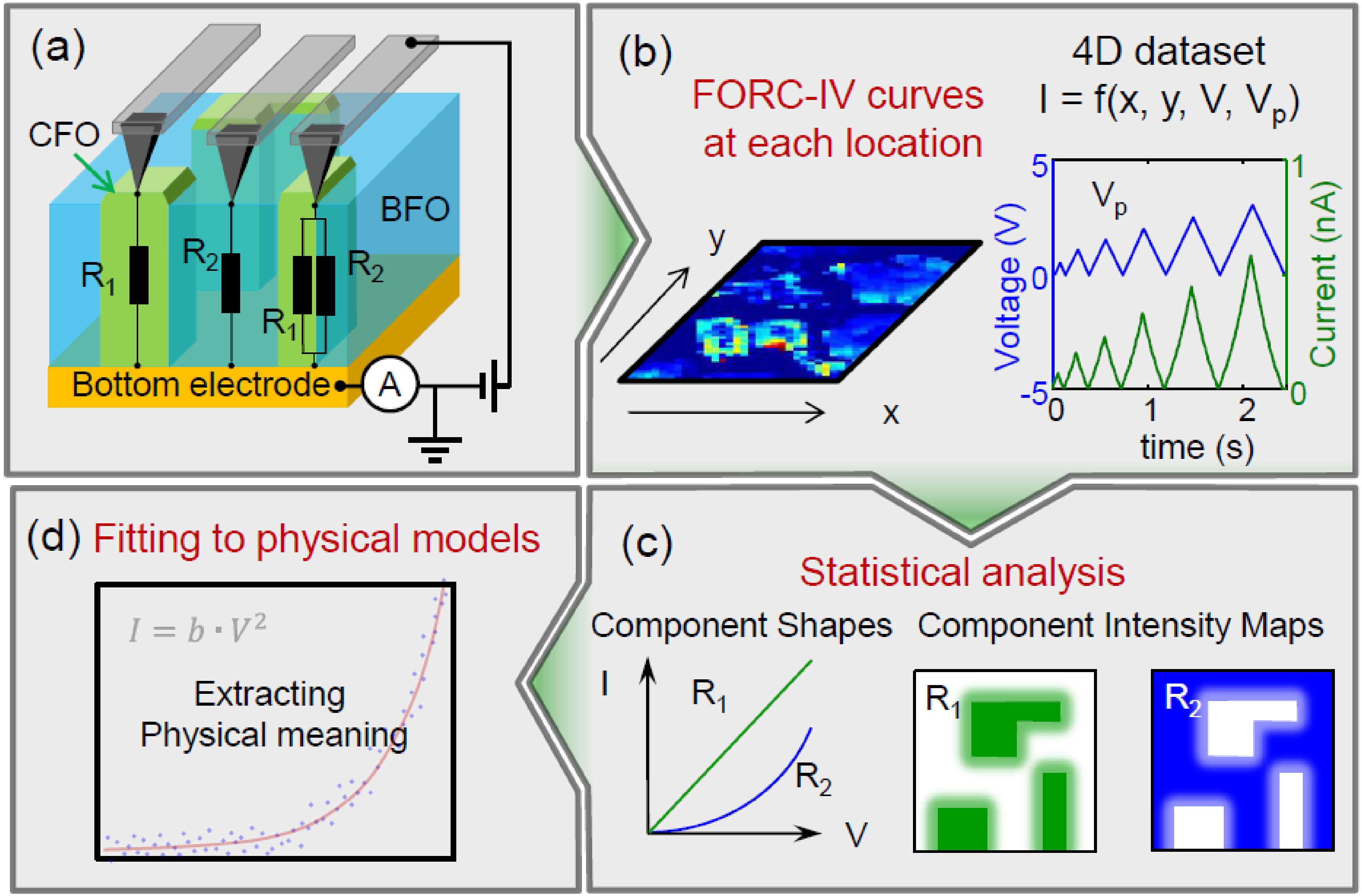

Wait, there is more!

We need un-mixing/decomposition that are infused in some universal manner with a priori physical information (trivial example is constraints, a less trivial one is a simulation of some expected components) s that the resultant components can be directly interpreted in physical terms.

For example:

- Bayesian linear unmixing: constraints on endmembers
- Sparse reconstructions: small number of components in each point
- Constraints on loading maps: smoothness or sharp boundaries
- Kernel transforms: data is simplest if physics is correct